



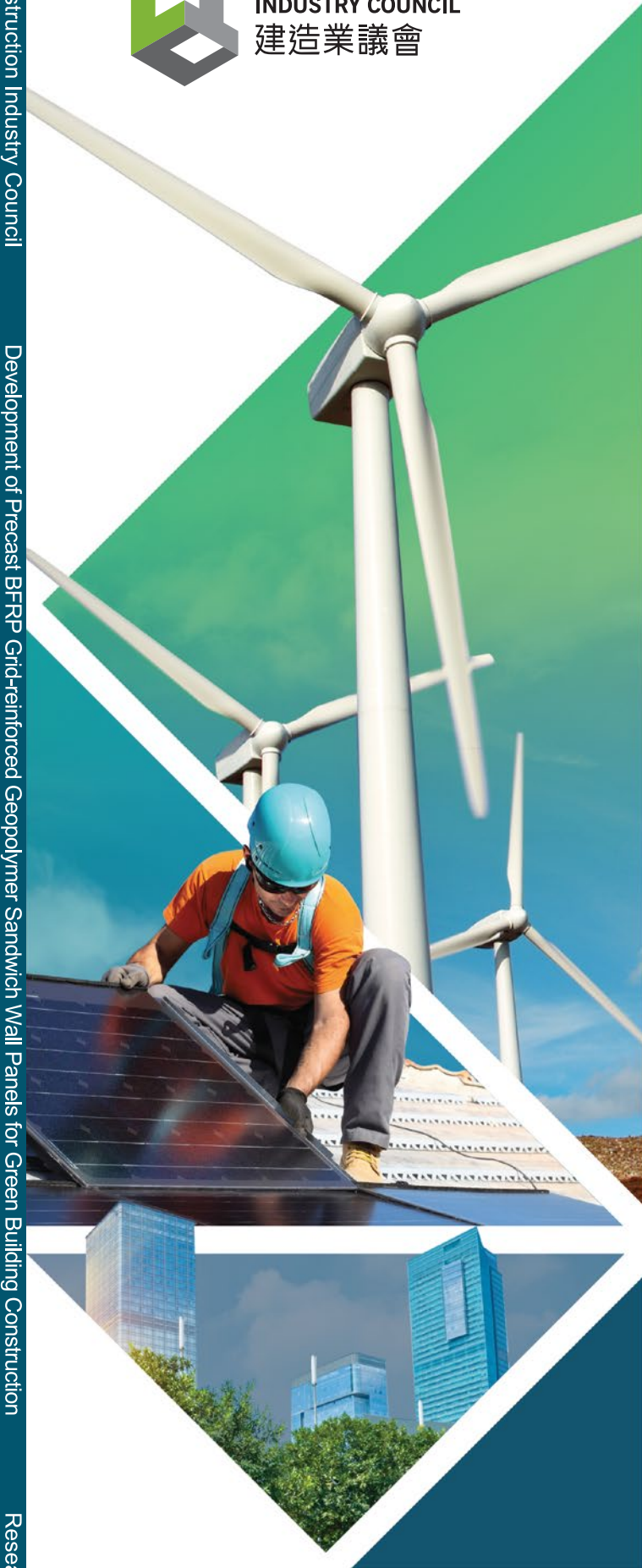
CONSTRUCTION
INDUSTRY COUNCIL
建造業議會

DEVELOPMENT OF PRECAST BFRP GRID-REINFORCED GEOPOLYMER SANDWICH WALL PANELS FOR GREEN BUILDING CONSTRUCTION

Construction Industry Council

Development of Precast BFRP Grid-reinforced Geopolymer Sandwich Wall Panels for Green Building Construction

Research Summary



RESEARCH SUMMARY



Author

Prof. Jian-Guo DAI
The Hong Kong Polytechnic University

Published by

Construction Industry Council,
Hong Kong SAR

DISCLAIMER

The information given in this report is correct and complete to the best of knowledge of the authors and publisher. All recommendations are made without guarantee on the part of the authors or publisher. The authors and publisher disclaim any liability in connection with the use of the information given in this report.

Enquiries

Enquiries on this research may be made to the CIC Secretariat at:

CIC Headquarters
38/F, COS Centre, 56 Tsun Yip Street, Kwun Tong, Kowloon

Tel.: (852) 2100 9000

Fax: (852) 2100 9090

Email: enquiry@cic.hk

Website: www.cic.hk

© 2018 Construction Industry Council.



FOREWORD

Precast concrete elements have been widely adopted for construction in Hong Kong. While sandwich panels, which can be structural and non-structural components, are fire-resistant, durable and energy efficient.

While the connectors of sandwich panels have been modified from concrete block and steel bent-up bar to fiberreinforced polymers (FRP) to improve the energy efficiency, little study was carried out on how the FRP connectors influence the structural performance. Hence, the CIC initiated the research by engaging a research team from The Hong Kong Polytechnic University to investigate the structural performance.

The research work presented in this report was funded by the CIC Research Fund, which was set up in September 2012 to provide financial support to research institutes/construction industry organizations to undertake research projects which can benefit the Hong Kong construction industry through practical application of the research outcomes. CIC believes that research and innovation are of great importance to the sustainable development of the Hong Kong construction industry. Hence, CIC is committed to working closely with industry stakeholders to drive innovation and initiate practical research projects.

The research work described in the report was carried out by a research team led by Prof. Jian-Guo DAI from The Hong Kong Polytechnic University. The project cannot succeed without the dedicated effort of the research team. I would like to thank to all who took part in this valuable work.

Ir Albert CHENG

Executive Director

Construction Industry Council



PREFACE

The use of innovative materials and structures has become an important dimension of the construction industry. The Department of Civil and Environmental Engineering (CEE) at the Hong Kong Polytechnic University has a worldwide reputation in frontier researches relevant to the use of emerging materials and structural systems for achieving longevity and sustainability of buildings and civil engineering infrastructures. In particular, PolyU's CEE plays a world leading role in the research areas of fiber-reinforced polymer (FRP) composites in construction and eco-friendly concrete technology.

The research project reported here is a good example demonstrating the Department's research strength in the above-mentioned research areas. This project focused on the development of a new type of sandwich load-bearing wall panel system enabled by fiber-reinforced polymer (FRP) connectors, which has great potentials for application in the prefabrication industry in Hong Kong. The prefabricated sandwich system is featured with the following innovations: (1) geopolymer cement concrete (i.e., alkali-activated industry byproducts like fly ash and slag) is used to replace ordinary Portland cement concrete to construct the interior and exterior wythes of the sandwich wall, so that industrial wastes can be efficiently used and the carbon footprint can be significantly reduced; (2) an innovative tubular connector made of fiber-reinforced polymer (FRP) composites, which are non-corrosive, light and strong, is used to facilitate the composite action of the sandwich wall and to improve the energy efficiency.

I would like to congratulate my colleague Ir Prof. Jian-Guo DAI and his research team for accomplishing this important research project. On behalf of the Department, I would also like to sincerely thank the CIC for its financial support. I am confident that the completion of this project will further strengthen the collaborations between PolyU and the local industry and add essential values to the prefabricated building industry in Hong Kong.

Ir Prof C.S. POON

Head, Department of Civil and Environmental Engineering
The Hong Kong Polytechnic University

RESEARCH HIGHLIGHTS

Precast concrete sandwich panels (PCSPs) have been widely used as the facade walls and load bearing walls in practical engineering. They mainly consist of inner and outer reinforced concrete wythes, core insulation wythes and connectors penetrating through the insulation. Depending on the stiffness, resistance, and distribution of the connectors, the PCSPs are classified as fully composite, partially composite and non-composite types. In this project, a new type of PCSP system consisting of two exterior wythes made by FRP-reinforced geopolymer concrete and a glass FRP (GFRP) connector is proposed. The structural behaviours of the proposed new PCSP system were studied within the following contexts: (1) the individual performance of three types of the proposed GFRP connectors (i.e., flat plate, corrugated plate, and hexagonal tube connector); (2) structural performance of steel reinforced geopolymer concrete one-way slab; (3) structural performance of basalt FRP (BFRP) reinforced geopolymer concrete one-way slab; (4) structural performance of precast geopolymer concrete sandwich panels (PGCSP); (5) a simplified approach for predicting the deflection of PCSP; and (6) fire performance of the proposed PCSP. Upon the completion of the project, an in-depth understanding of the mechanical performance of the proposed PCSP system has been achieved. The proposed PCSP system is expected to have great potential for applications in prefabricated building industry due to its improved durability, environmental friendliness and energy efficiency, which comply well the sustainability policy being promoted by the Hong Kong construction industry.

CONTENTS

1	INTRODUCTION	1
1.1	Background	1
1.2	Aims and Objectives	2
1.3	Scope	3
2	DEVELOPMENT OF GFRP CONNECTORS	4
2.1	Details of the Proposed GFRP Connectors	4
2.2	Research Methodology	5
2.3	Results	8
3	STRUCTURAL PERFORMANCE OF REINFORCED GEOPOLYMER CONCRETE ONE-WAY SLAB	11
3.1	Flexural Performance of Steel Reinforced Geopolymer Concrete One-way Slab	11
3.2	Shear Performance of BFRP Reinforced Geopolymer Concrete One-way slab	15
4	STRUCTURAL PERFORMANCE OF PRECAST GEOPOLYMER CONCRETE SANDWICH PANELS	19
4.1	Structural Performance of Precast Geopolymer Concrete Sandwich Panels	19
4.2	A Simplified Approach for Stiffness and Serviceability Prediction of Precast Concrete Sandwich Panel	25
5	FIRE PERFORMANCE OF PRECAST GEOPOLYMER CONCRETE SANDWICH PANELS	29
5.1	Research Methodology	29
5.2	Results	31
6	CONCLUSIONS AND FURTHER RESEARCH	33
6.1	Conclusions	33
6.2	Further Research	34
7	REFERENCES	35
	APPENDIX	37
	Brief Guideline for Design of Precast Geopolymer Concrete Sandwich Panel Reinforced by BFRP Rebar	37

1 INTRODUCTION

1.1 Background

Precast concrete structural members are widely used in construction industry. They have many advantages over cast-in-place concrete members such as high quality control, short construction period, and reduction of construction waste (Lacerda *et al.* 2018). Recently, the application of precast construction has been a trend particularly in Hong Kong and Mainland China.

Precast concrete sandwich panels (PCSPs) as the typical structural element in precast industry, have been widely used as the facade walls or load-bearing walls in engineering practice. The components of a PCSP are inner and outer reinforced concrete (RC) wythes, core insulation and connectors penetrating through the insulation. Depending on the stiffness and strength performance, the PCSPs are classified into three categories: fully composite, partially composite and non-composite. (PCI committee 2011). The fully composite PCSP means that the two RC wythes act as one panel. The non-composite PCSP means that the two RC wythes operate independently, and partially composite PCSP lies between the two mentioned extreme mechanical behaviors. Traditionally, concrete block and steel bent-up bar were used as the connectors (Bush and Stine 1994; Bush and Wu 1998; PCI Committee 2011), which could achieve a high degree of composite action (in terms of stiffness and strength). However, they were prone to thermal bridge effect which could occur due to the higher thermal conductivity of steel and concrete. Such a deficiency usually reduces the energy efficiency of the entire sandwich panel. Therefore, fiber-reinforced polymers (FRPs) recently have been used as the connectors due to their high strength but low thermal conductivity (Einea *et al.* 1994; Pantelides *et al.* 2008; Hassan and Rizkalla 2010; Frankl *et al.* 2011; Naito *et al.* 2012; Al-Mahaidi *et al.* 2013; Woltman *et al.* 2013; Hodicky *et al.* 2015). However, limited investigations have been conducted on how the FRP connectors influence the structural performance of the fabricated PCSPs. In addition, most existing FRP connectors were designed to transfer one-directional shear force and the formed PCSPs were usually non-composite type due to the lower stiffness and lower capacity of the connectors. According to the explored background, this report is concerned with the development of a new type of PCSP.

1.2 Aims and Objectives

In this report, a new PCSP system is proposed. In this system, geopolymer concrete is adopted to replace Ordinary Portland Cement (OPC) to construct the two wythes. Geopolymer is an inorganic binder which adopts industrial by-products as the dry materials (Davidovits, 1991). Those by-products are rich in silica and aluminum (e.g. blend of fly ash and slag). The geopolymer is formed by reacting the dry material with alkaline activator, and this process is called geopolymerization. The mechanical property of the geopolymer is comparable to that of the OPC (Fernándezjiménez *et al.* 2006) with the merit of producing 50 – 80% greenhouse gas (CO₂) emission lower than that of OPC (Duxson *et al.* 2007; Provis and Van Deventer 2009). On the other hand, in the new system, FRP rebar is used to replace steel rebar to improve the durability and to minimize the thickness of the entire panel. In addition, a tubular glass FRP (GFRP) connector was developed to enhance the composite action of the PCSP. Thus, the proposed PCSP system not only retains the energy efficiency of the existing PCSPs but possesses the following innovative features:

- (1) By replacing the OPC concrete with the geopolymer concrete, the resultant PCSP would be much more environmental friendly than before;
- (2) Durability would be enhanced by replacing steel rebar with FRP rebar;
- (3) Structural efficiency would be further enhanced by using the developed FRP connector.

The following objectives were primarily addressed in this report:

- (1) A new type of GFRP tubular connector was devised and its mechanical performance was investigated;
- (2) The structural performance of steel and FRP-reinforced geopolymer concrete one-way slabs which act as the two wythes in the PCSP system was evaluated;
- (3) The structural performance of the GFRP connector-enabled precast geopolymer concrete sandwich panel (PGCSP) was investigated. Then a simplified approach was developed for predicting the stiffness and serviceability of the PCSP under out-of-plane load;
- (4) The fire performance of the GFRP connector-enabled PGCSP was investigated.

1.3 Scope

The project started in the first of January 2015 and lasted by the end of August 2018. The four aforementioned objectives were addressed by conducting extensive experimental and finite element (FE) analyses. The details are outlined in the following.

- (1) Twenty-five in-plane direct shear tests were conducted to evaluate the effect of GFRP laminate thickness, projected length, and shear force direction on the performance of three types of GFRP connectors (i.e., flat plate, corrugated plate and hexagonal tube). The shear force vs. relative slip relationships and failure modes of all types of connector were studied and discussed. Besides, three-dimensional (3D) FE analysis was conducted to reproduce the test results, aiming to facilitate an in-depth understanding of the failure mechanisms and the full-range performance of the connectors.
- (2) Six steel reinforced geopolymer concrete one-way slabs and six OPC concrete counterparts were tested under four-point flexural load. The shear performance of six basalt FRP (BFRP) reinforced geopolymer concrete one-way slabs were also evaluated. The investigated parameters were concrete strength and reinforcement ratio. The load-deflection relationships, crack patterns, failure modes of the samples were studied and compared. Meanwhile, two-dimensional (2D) FE analysis was conducted to reproduce the test results to fully understand the behaviour of the reinforced geopolymer concrete slabs as the two wythes in the PCSP system.
- (3) An experimental study was carried out on the flexural performance of eight PGCSPs. Four parameters were investigated, including the connector type (i.e., plate-type and hexagonal tube connector), connector spacing, rebar type (i.e., steel and BFRP rebar) and reinforcement ratio. The load-deflection relationships, crack patterns, failure modes and degrees of composite action (in terms of both stiffness and strength) of the specimens were carefully investigated. In addition, 2D FE analysis incorporating the shear-slip constitutive laws of FRP connectors was conducted to reproduce the test results. A simplified but innovative approach (with closed-form solutions) based on the continuum method was developed for predicting the stiffness and serviceability of the PCSP under out-of-plane load. The proposed approach was validated by the tests.
- (4) Five PCSP specimens were fabricated and tested under one-side fire condition. The investigated parameters were the concrete type (geopolymer and OPC concrete), the reinforcement type (steel and BFRP rebar), the connector type (plate-type and hexagonal tube GFRP connector), and the concrete wythe thickness (75 and 100 mm). The temperature distributions, the deformation responses, the failure modes, and the fire resistances of all specimens were studied and compared in detail.

2 DEVELOPMENT OF GFRP CONNECTORS

2.1 Details of the Proposed GFRP Connectors

Fig. 1a~c shows the three proposed GFRP connectors and their connection details in PCSPs. The flat and corrugated plate connectors were mainly proposed as one-way connectors (i.e., designed to transfer one-way shear force). The flat plate connector is a typical plate-type connector that may fail in buckling, especially when the thickness of GFRP laminate is small. A corrugated plate GFRP connector was also explored (Fig. 1b) which can delay or avoid the buckling. The hexagonal tube GFRP connector was mainly proposed as a two-way connector (i.e., designed to transfer two-way shear force). Compared with a solid section, the tubular section is expected to be optimal because it provides higher bending/transverse stiffness under flexure/shear load in PCSPs. In fact, both shear and flexural deformations occur when the connector is subjected to a shear force, although previous studies usually refer to them as “shear connectors” (PCI Committee 2011). Based on the existing manufacturing facilities in the lab and considering the convenience for manufacturing, GFRP tubes with a hexagonal section were first proposed. For all of the connectors, a reliable anchorage system was achieved by penetrating the reinforcing bars in the two wythes by the predrilled holes at the top and bottom of each connector.

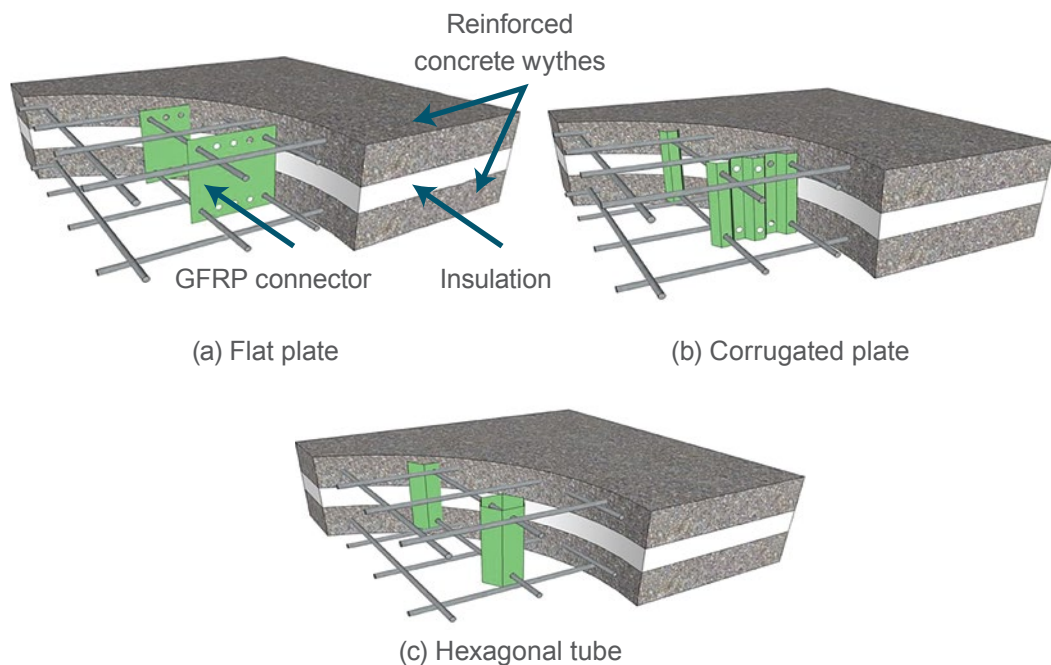


Figure 1 PCSP with the proposed connector

2.2 Research Methodology

The performance of the proposed GFRP connectors was investigated experimentally and numerically. For the experiment investigation, twenty-five specimens were tested under in-plane direct shear with two identical specimens for each combination of test parameters. For the flat and corrugated plate connectors, the investigated parameters were the projected length (100 and 160 mm) and the thickness (two and four plies of glass fiber sheet). For the hexagonal tube connector, the investigated parameters were shear force direction (X and Y direction in Fig. 2c) and thickness. Figure 2a~c show the configuration and shear force direction of the connectors. Twenty-four of the specimens were named in the form of T-S-P-1&2, where “T” refers to the connector type (symbolized as “F,” “C,” and “H” for the flat plate, corrugated plate, and hexagonal tube connector, respectively); “S” refers to the projected length (symbolized as “100” and “160” mm) and the shear force direction (symbolized as “X” and “Y”) for the one- and two-way connectors, respectively; and “P” refers to the thickness of the GFRP laminate (symbolized as “2” or “4” plies). The final specimen (i.e., H-Y-4NB) had the same combination of test parameters with specimen H-Y-4, while a plastic sheet was attached on the insulation surface to eliminate the bond between the concrete and the insulation. The overall dimensions of the test specimens were 400×300×300 mm (i.e., length×width×height) which represented a two back-to-back sandwich panel. Fig. 2d shows the details of the specimen geometry. In the specimens, extruded polystyrene (XPS) foam with a smooth surface condition was used as the insulation layer. The thickness of the insulation was 50 mm. In order to measure the relative slip between the core concrete wythe and the two outer concrete wythes, the linear variable differential transformers (LVDTs) were placed at the front and back of each concrete wythe. The load was applied in a displacement-controlled manner at a loading rate of 1 mm/min. A load cell was placed at the top center of the core concrete wythe to measure the load.

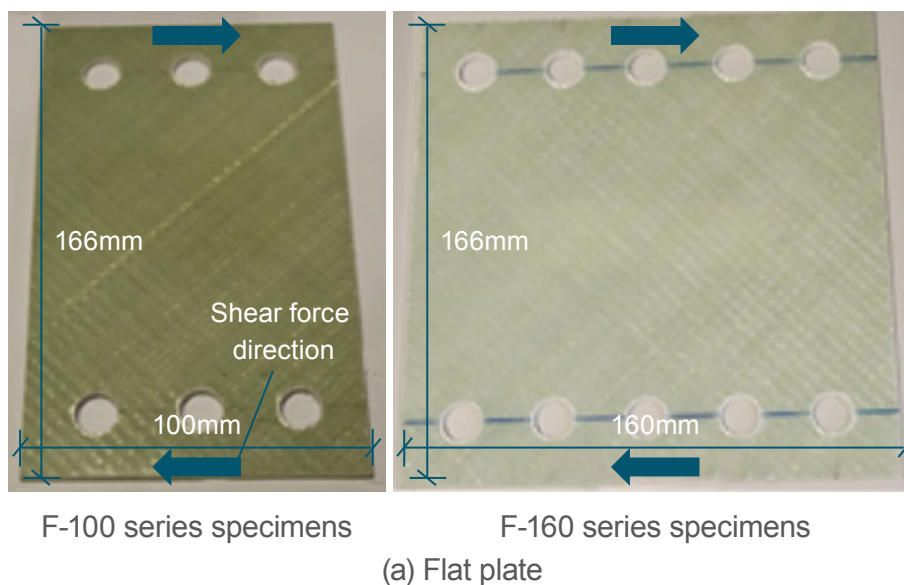
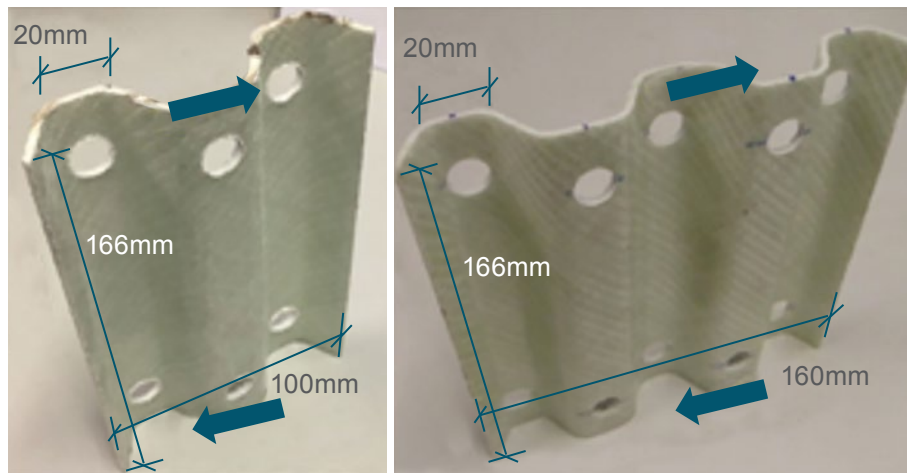


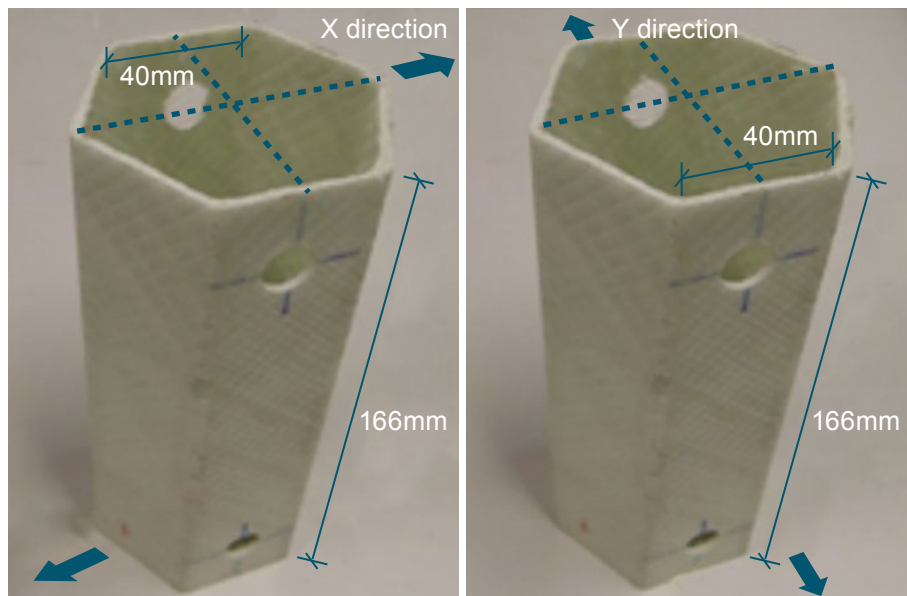
Figure 2 Geometry of proposed GFRP connectors and test setup



C-100 series specimens

C-160 series specimens

(b) Corrugated plate



H-X series specimens

H-Y series specimens

(c) Hexagonal tube

Figure 2 Geometry of proposed GFRP connectors and test setup

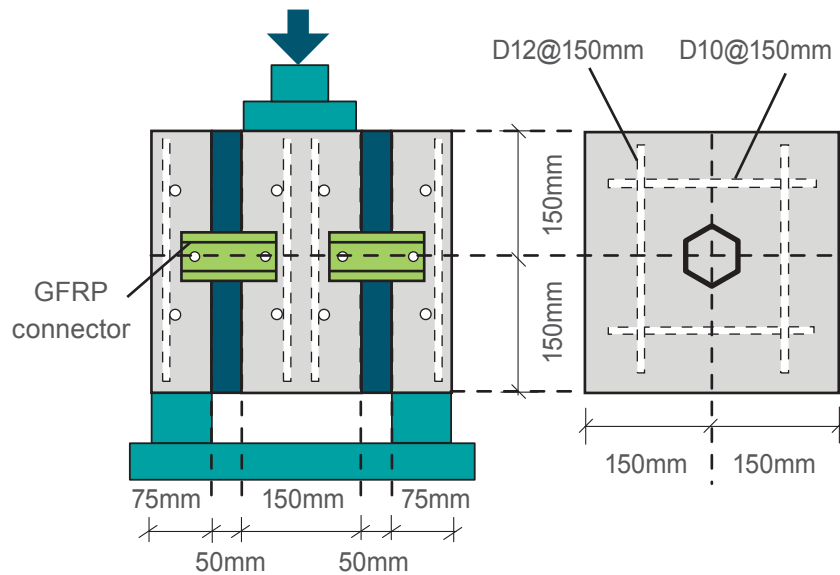


Figure 2 Geometry of proposed GFRP connectors and test setup

Furthermore, 2D FE analysis was conducted to reproduce the initial linear and the non-linear behavior of the in-plane direct shear test. A general-purpose FE program known as ABAQUS (2010) was used. Due to the symmetry, only half of the model was analyzed. An eight-node solid element (C3D8R) was used to simulate two concrete wythes. A shell element (S4R) was used to model the GFRP laminate, with four and eight layers for two and four plies of glass fiber sheet, respectively. Damages in the GFRP laminate were considered in the FE model through Hashin damage model. The overall view of the FE model is shown in Fig. 3. Here, a perfect bond was assumed between the concrete and the connectors.

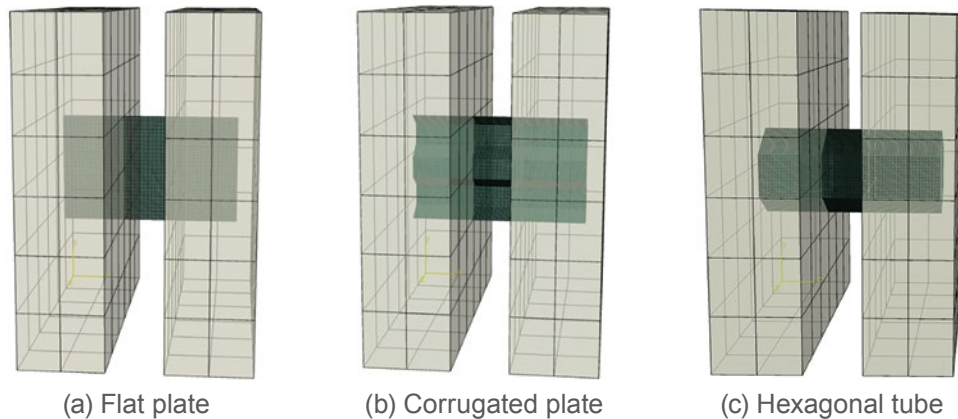


Figure 3 FE model of the direct shear test specimen

2.3 Result

The solid lines in Fig. 4a~f represent the average shear force vs. relative slip relationship related to two identical specimens. The average shear force was obtained by averaging the shear force values of the two identical specimens at each specific relative slip level. The transparent dash lines in the figures are the responses of each individual specimen. It is evident in the figures that all the GFRP connectors experienced a progressive failure. The corrugated section led to much improved deformability when the thickness was smaller, as shown in Fig. 4a~b. This was mainly due to the premature buckling of the flat plate connectors. When the GFRP laminate thickness increased into four plies, the buckling did not occur even in the F series specimens, although the deformability was still slightly inferior to that of the C series specimens (Fig. 4c~d). From Fig. 4e~f, the H-X and H-Y specimens show similar responses, indicating that the hexagonal tube GFRP connectors had similar performances along the two directions. Meanwhile, H-Y-4NB presented a similar shear force vs. relative slip relationship to that of H-Y-4, as shown in Fig. 4f. Thus, it is reasonable to conclude that the insulation had no contribution to the shear stiffness and the shear force resistance. The obtained shear force vs. relative slip curves reflected only the performance of the GFRP connectors.

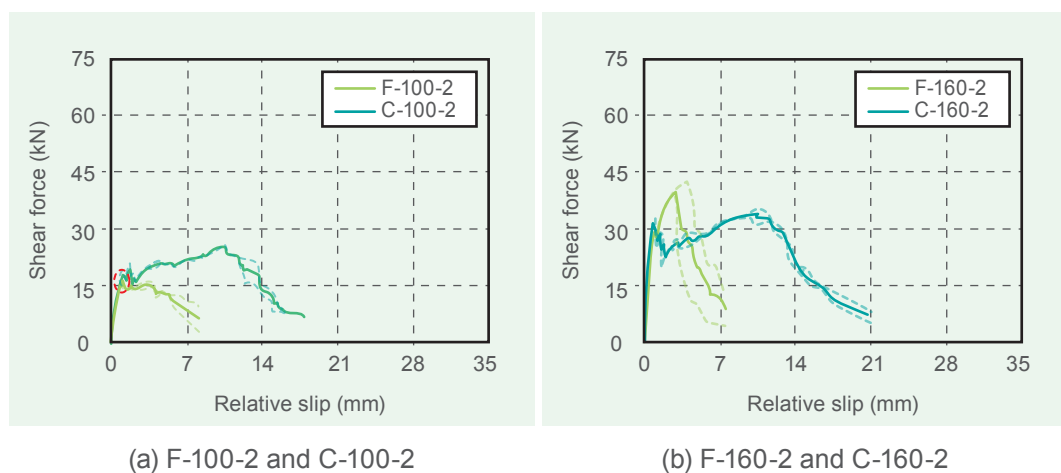


Figure 4 Shear force vs. relative slip relationships of the direct shear test specimens

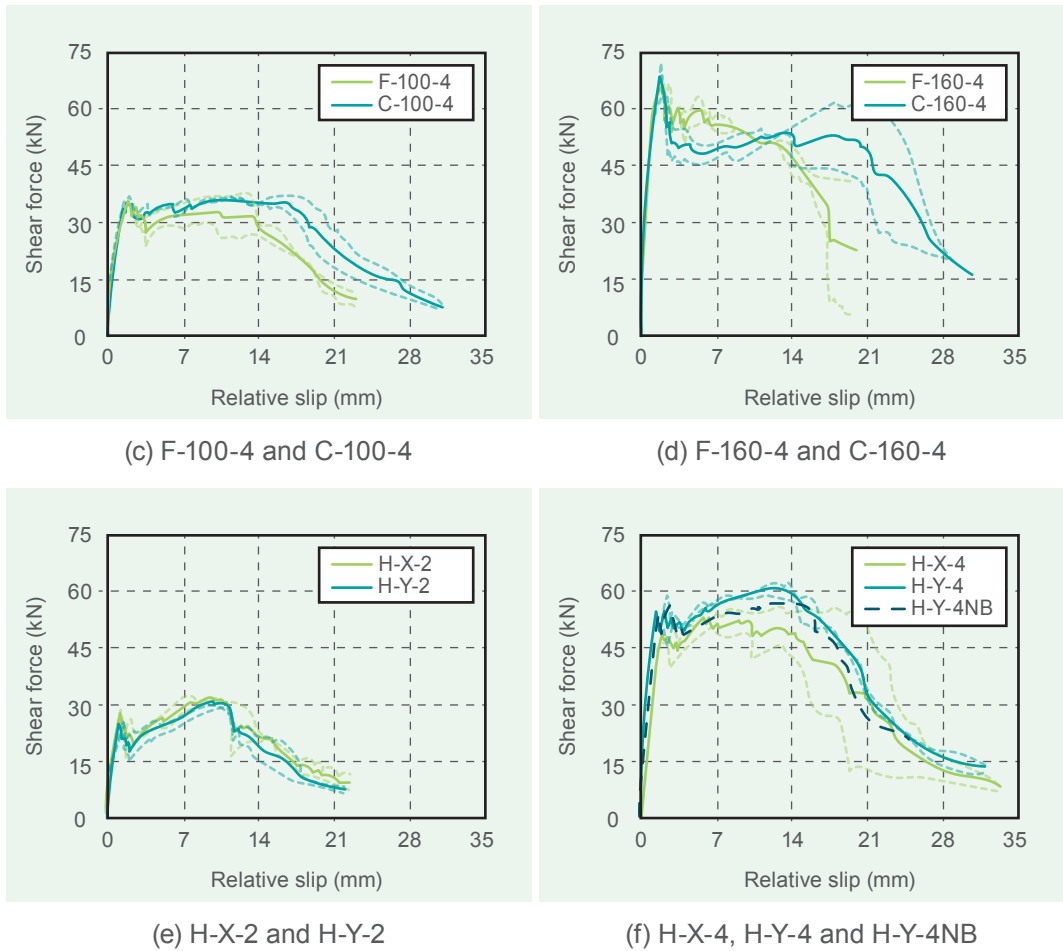
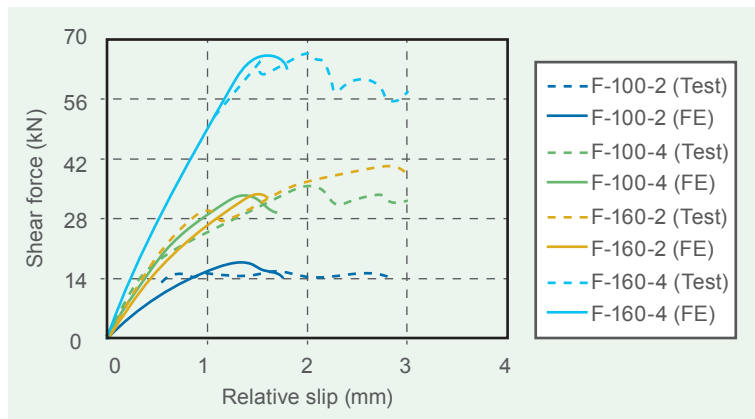
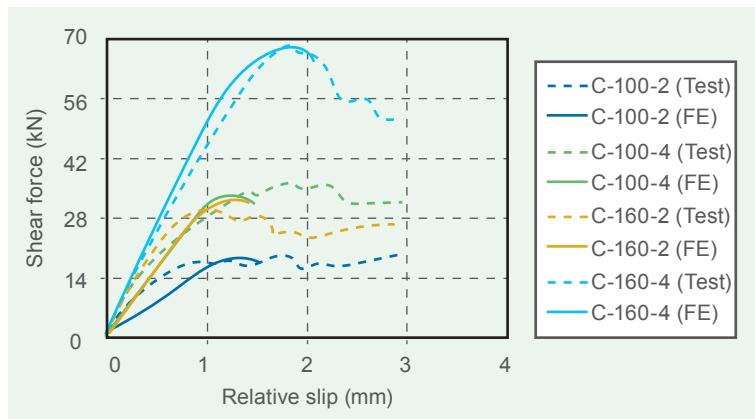


Figure 4 Shear force vs. relative slip relationships of the direct shear test specimens

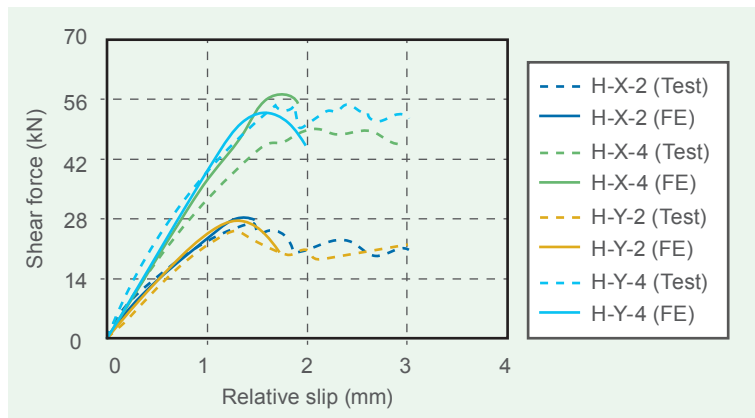
Fig. 5 compares the shear force vs. relative slip relationships between the FE analysis and the test results. The FE results fit well with the test results in terms of the ascending part. However, the FE model could not capture the post-peak behavior, probably due to adopted smeared approach. The analysis was stopped after the load reached the peak load. However, the FE model could give reasonably accurate predictions for the initial secant stiffness of the connector and the load resistance.



(a) F series specimens



(b) C series specimens



(c) H series specimens

Figure 5 Comparison of shear force vs. relative slip relationships between test and analysis results

3 STRUCTURAL PERFORMANCE OF REINFORCED GEOPOLYMER CONCRETE ONE-WAY SLAB

3.1 Flexural Performance of Steel Reinforced Geopolymer Concrete One-way Slab

3.1.1 Research Methodology

The flexural performance of steel reinforced geopolymer concrete one-way slabs was investigated experimentally. A total of twelve RC slabs were fabricated and tested. The geometry of the specimens was 2100×500×120 mm (length×width×depth). Six of them were made of geopolymer concrete having three concrete strength levels (around 30, 40 and 50 MPa) and two different reinforcement ratios (0.82% and 1.20%). Different reinforcement ratios were obtained by using two longitudinal rebar diameters (10 mm and 12 mm). In parallel, the other six slabs were made of OPC concrete. All the specimens were symbolized in the form of T-D-C, where “T” refers to the concrete type (“GCS” and “OCS” for geopolymer and OPC concrete slab, respectively); “D” refers to the diameter of longitudinal rebar (i.e., “10” and “12” mm); and “C” refers to the concrete compressive strength (i.e., “30”, “40” and “50” MPa). All specimens were reinforced by 10 mm diameter transverse rebar at a space of 200 mm. The concrete cover remained constant at 20 mm.

The specimens were tested under four-point flexural loading condition. The lengths of the shear span and constant moment zone were all 640 mm. Fig. 6 shows the photo of the test setup. LVDTs were placed to measure the deflection at the mid-span and two loading points. The load was applied by a hydraulic jack.

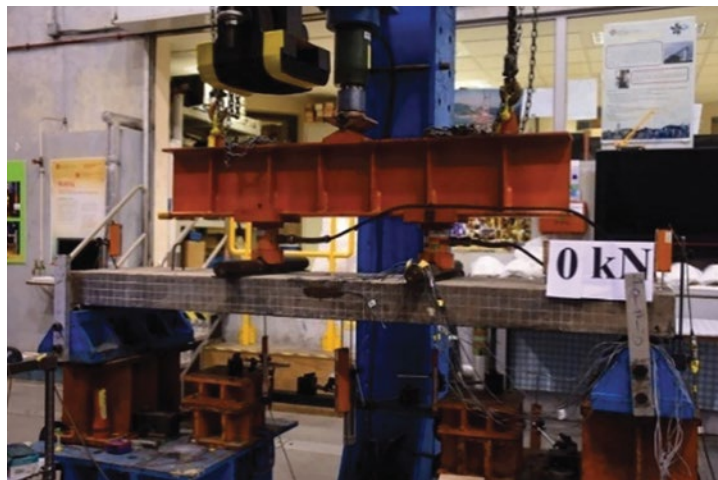
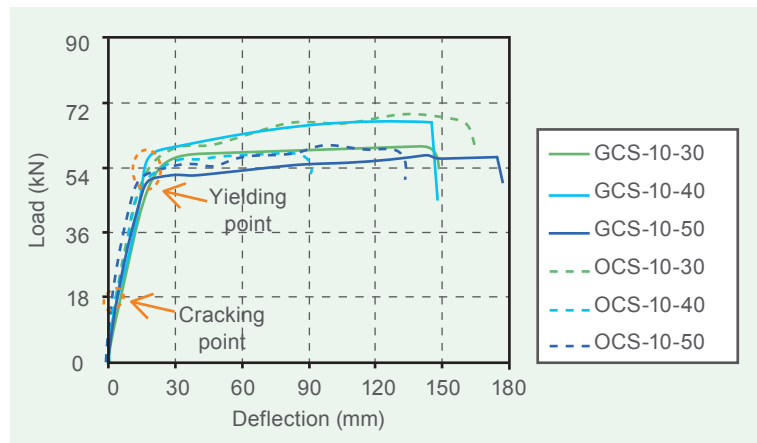


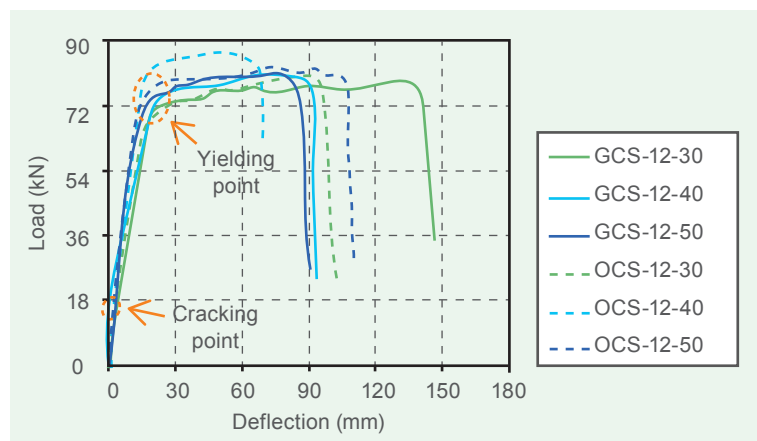
Figure 6 Test setup of the reinforced concrete one-way slab

3.1.2 Results

The load vs. mid-span deflection relationship of the specimens is shown in Fig. 7. It seems that for the GCS specimens the initial and post-cracking stiffness, cracking load, yielding load and load carrying capacity are similar to those of the OCS counterparts. The failure mode and crack pattern of GCS-12-50 and OCS-12-50 are shown in Figure 8(a) and (b), respectively. Both mentioned samples presented a concrete crushing failure at the top surface of the constant moment zone. In summary, the flexural performance of steel rebar reinforced geopolymer concrete one-way slabs are similar to that of the OPC concrete counterparts.



(a) Specimens with lower reinforcement ratio



(b) Specimens with higher reinforcement ratio

Figure 7 Load vs. mid-span deflection relationship of the test steel rebar reinforced one-way slab specimens

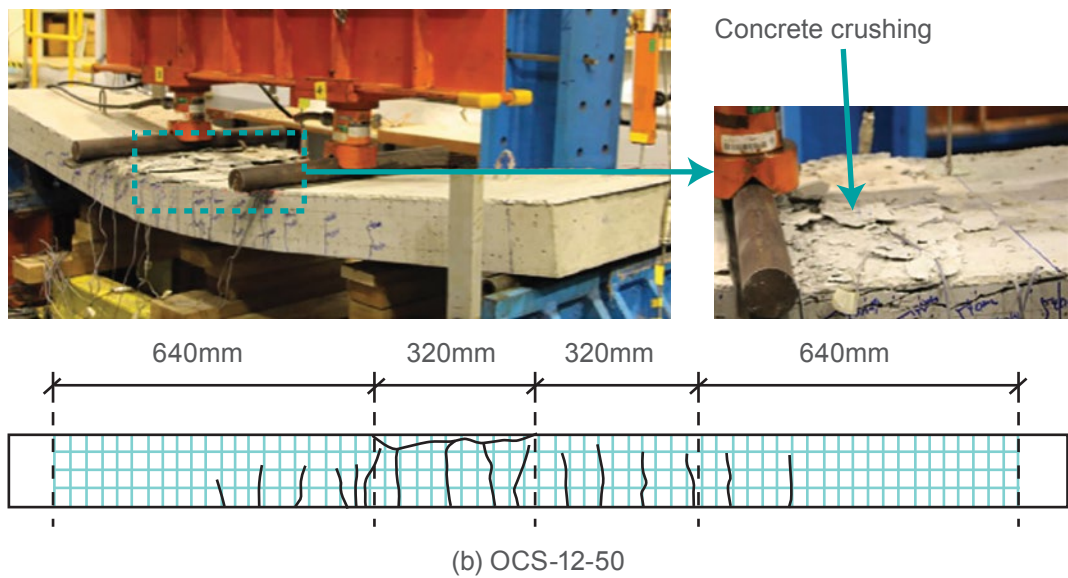
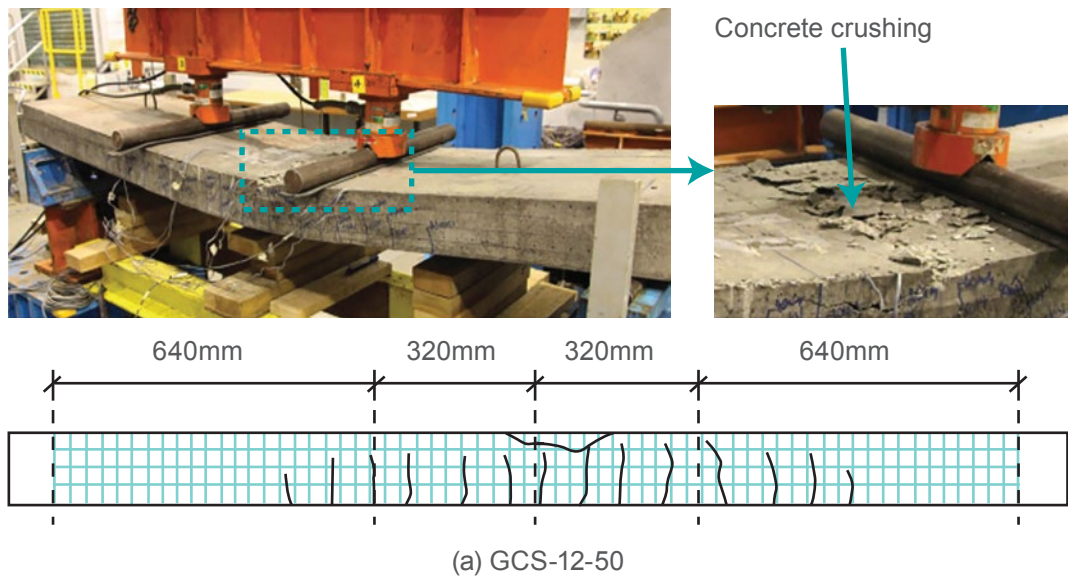


Figure 8 Failure mode and crack pattern of GCS-12-50 and OCS-12-50

Design provisions (ACI-318-05 (2005) and GB50010-2010 (2010)) were used to predict the cracking loads and the load carrying capacities of the GCS specimens. Their loads at the service limit state (i.e., the deflection limit of $l/180$ and $l/200$ for ACI-318-05 and GB50010-2010, respectively) were also evaluated. The results were shown in Table 1. By ACI 318-05 and GB50010-2010, the average ratios between the predicted and the tested cracking loads were 0.89 (0.77 – 1.01) and 0.95 (0.76 – 1.12), respectively. The average ratios between the predicted and the measured load carrying capacities were 0.82 for both ACI-318-05 and GB50010-2010. These results indicated that the design provisions had the potential to be used for calculating the cracking load and the load carrying capacity in design of the steel reinforced geopolymer concrete one-way slabs. Also, the GCS specimens could maintain around half of the load carrying capacity at the service limit state.

Table 1 Comparison of the cracking load, load at service limit state and load carrying capacity

Specimen ID	Cracking load (kN)			Load at service limit state (kN)			Load carrying capacity (kN)		
	ACI	GB	Test	$l/200$	$l/180$	$\omega=0.2$ mm	ACI	GB	Test
GCS-10-30	13.0 [0.85]	12.8 [0.84]	15.3	30.1 (0.50)	33.1 (0.54)	37.7 (0.62)	46.5 [0.76]	47.0 [0.77]	60.8
GCS-12-30	13.0 [0.77]	12.8 [0.76]	16.8	38.3 (0.48)	41.1 (0.52)	48.9 (0.61)	70.8 [0.89]	72.1 [0.90]	79.8
GCS-10-40	15.1 [0.85]	16.9 [0.95]	17.7	35.3 (0.52)	37.7 (0.56)	40.2 (0.60)	47.4 [0.70]	47.7 [0.71]	67.5
GCS-12-40	15.1 [0.92]	16.9 [1.03]	16.4	37.4 (0.46)	40.5 (0.50)	45.2 (0.56)	73.0 [0.91]	73.8 [0.82]	80.5
GCS-10-50	16.7 [1.01]	18.6 [1.12]	16.6	32.8 (0.57)	36.0 (0.62)	34.5 (0.59)	45.0 [0.78]	45.2 [0.78]	58.0
GCS-12-50	16.7 [0.92]	18.6 [1.03]	18.1	46.1 (0.57)	50.6 (0.62)	44.1 (0.54)	70.4 [0.86]	70.9 [0.87]	81.5

Note: () represents the ratio between the load at service limit state and the tested load carrying capacity;
 [] represents the ratio between predicted and tested cracking loads or load carrying capacities;
 l is the length between two supports.

3.2 Shear Performance of BFRP Reinforced Geopolymer Concrete One-way slab

3.2.1 Research Methodology

The shear performance of BFRP reinforced geopolymer concrete one-way slab was investigated both experimentally and numerically. For the experiment, six BFRP rebar reinforced geopolymer concrete one-way slabs were fabricated and tested. The geometry of the specimens was 2100×500×120 mm (length×width×depth). The investigated parameters were the concrete compressive strength (approximate 30, 40 and 50 MPa) and reinforcement ratios (1.20% and 2.18%). Different reinforcement ratios were achieved by changing longitudinal rebar diameter (12 and 16 mm). The out-of-plane shear performance of the specimens were evaluated by four-point flexural loading test. The specimens were termed in the form of GCS-R-C, where “R” refers to the longitudinal reinforcement type (symbolized as “B12” and “B16”, for longitudinal BFRP rebar diameter of 12 and 16 mm, respectively); and “C” refers to concrete compressive strength (symbolized as “30”, “40” and “50” MPa). The test setup and instruments were the same as those in Fig. 6.

The FE analysis was conducted in ABAQUS. The overall view of a FE model is found in Fig. 9. Here, four-node plane stress element (CPS4R) was adopted for modelling concrete and the loading pad. Two-node truss element (T2D2) was adopted for modelling the BFRP rebar. The BFRP rebar and the geopolymer concrete share the same nodes, which means the perfect bond between them. The slab had a simply supported boundary condition in which the translation degrees of freedom in X and Y direction were restricted at the left support, and the translation degree of freedom in Y direction was restricted at the right support. The load was added as the displacement on the loading points. The analysis was terminated after the load reached the peak value. Concrete damage plasticity model was used for modelling the non-linear behavior of the geopolymer concrete.

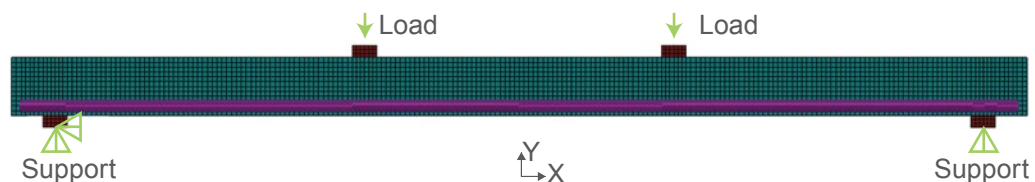


Figure 9 FE model of the BFRP reinforced geopolymer concrete one-way slab

3.2.2 Results

All tested BFRP reinforced geopolymer concrete one-way slabs presented a shear-compression failure. According to the load vs. mid-span deflection relationship shown in Fig. 10, all specimens had a load carrying capacity of 90.6~96.9 kN. Also, the post-cracking stiffness had an obvious increase with the increase of reinforcement ratio. The failure modes of GCS-B12-30 and GCS-B16-30 are shown in Fig. 11(a) and (b), respectively. Apparently, based on Fig. 11, the slab with lower reinforcement ratio properly maintained its integrity at the failure stage, whereas the slab with higher reinforcement ratio experienced severe splitting cracks.

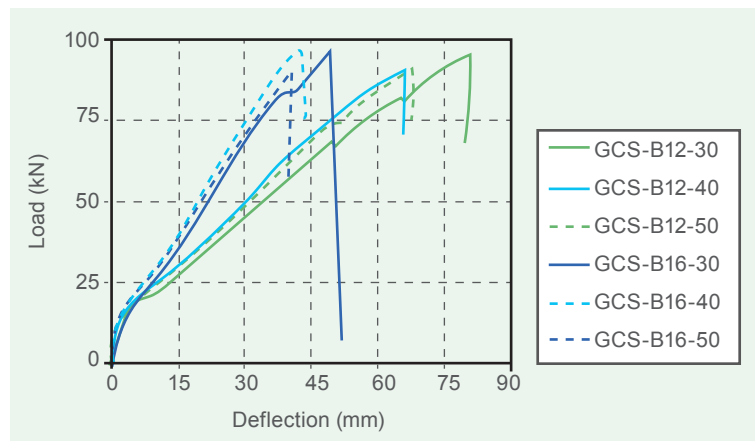
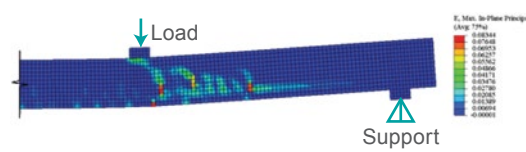
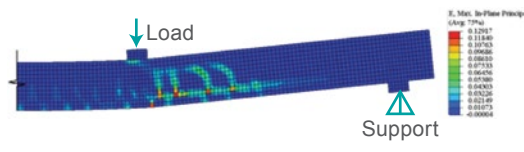
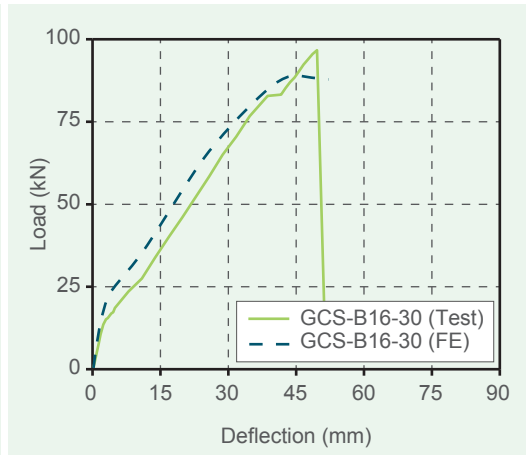


Figure 10 Load vs. mid-span deflection relationship of the BFRP reinforced geopolymer concrete one-way slabs



(a) GCS-B12-30

(b) GCS-B16-30

Figure 11 Comparison on the results of the BFRP reinforced one-way slab between test and FE analysis results



By the equations provided in ACI 440.1R-06 (2006), CAN/CSA-S806-12 (2012) and JSCE (1997), the shear resistances of the samples were predicted and compared with those of the tests. The ratios between the predicted and tested values are shown in Table 2. For ACI 440.1R-06, CAN/CSA-S806-02 and JSCE, the average ratios between the predicted and tested values were 0.54, 0.39, and 0.83, respectively. Therefore, the predicted results by the equations in ACI 440.1R-06 and CAN/CSA-S806-02 were too conservative. However, the JSCE shear design method provided an acceptable accuracy. Hence, the JSCE shear design method is recommended to be used in design of BFRP reinforced geopolymer concrete one-way slabs.

Table 2 Comparisons of the shear resistance between the test and calculated results

Specimen ID	Test (kN)	ACI 440.1R-06		CAN/CSA-S806-02		JSCE	
		Predict (kN)	Predict/test	Predict (kN)	Predict/test	Predict (kN)	Predict/test
GCS-B12-30	47.7	20.5	0.43	15.0	0.31	32.7	0.69
GCS-B12-40	45.3	22.4	0.50	16.7	0.37	36.5	0.81
GCS-B12-50	45.8	24.0	0.52	18.2	0.40	39.7	0.87
GCS-B16-30	48.5	25.2	0.52	17.4	0.36	36.5	0.75
GCS-B16-40	48.0	27.7	0.58	19.4	0.40	40.7	0.85
GCS-B16-50	45.0	29.7	0.66	21.1	0.47	44.3	0.98

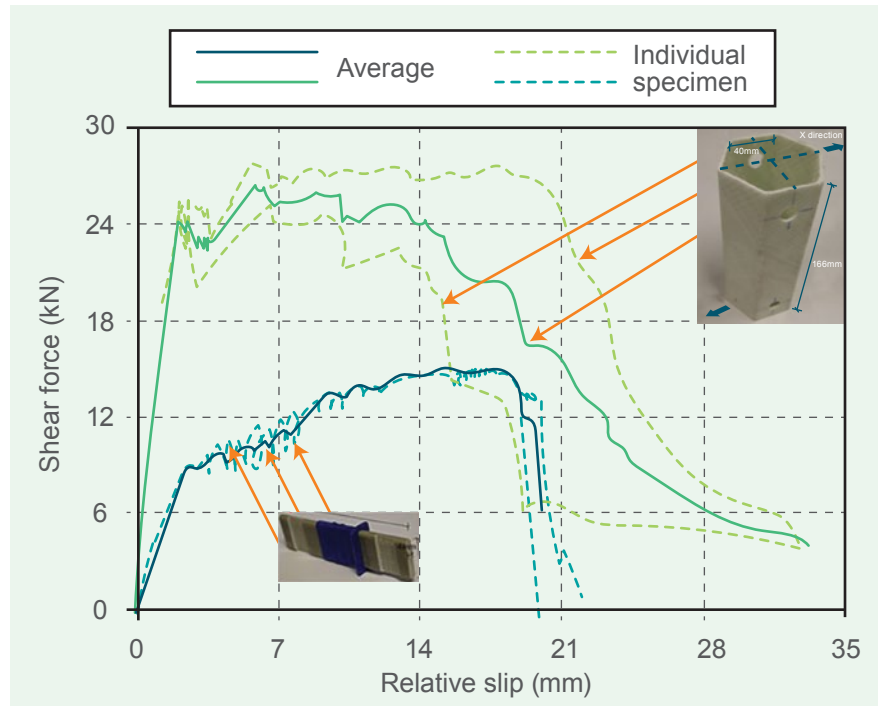
In Fig. 11, the load vs. mid-span deflection relationships of GCS-B12-30 and GCS-B16-30 are compared between the FE analysis and the tests. Generally, the predicted features such as the shape, the slopes and the maximum loads of the curves are comparable to the tests. The first principle strain contours of the models at the peak load are also shown in the figure. The contours adequately reflect the failure modes of the specimens, and fit well with the test observations. In summary, the proposed FE model was found useful for future applications as it provided reasonable predictions on the shear performance of the specimens.

4 STRUCTURAL PERFORMANCE OF PRECAST GEOPOLYMER CONCRETE SANDWICH PANELS

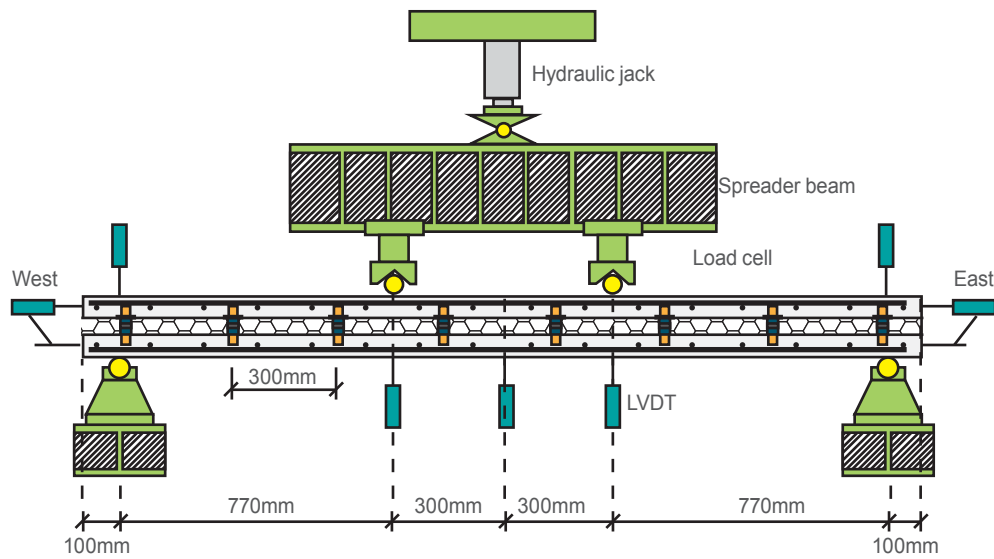
4.1 Structural Performance of Precast Geopolymer Concrete Sandwich Panels

4.1.1 Research Methodology

The structural performance of PGCSP was evaluated both experimentally and numerically. For the experiment, eight PGCSP specimens were fabricated and tested. The test specimen was a longitudinal unit of the sandwich wall panel with one column of the GFRP connectors. The geometry of the all specimens was 2340×300×200 mm (length×width×thickness). The outer concrete wythes was 75 mm thick and the core XPS insulation was 50 mm thick. The investigated parameters were the connector type (commercial plate-type and hexagonal tube GFRP connector), the connector spacing (300 mm and 525 mm), the rebar type (BFRP and steel rebar) and the reinforcement ratio (0.30% and 0.43%). Different reinforcement ratios were achieved by changing longitudinal rebar diameter (10 and 12 mm). Fig. 12a shows the shear force vs. relative slip relationship of the two adopted connectors. It was seen that the hexagonal tube connector presented a higher initial stiffness and shear resistance than those of the commercial plate-type connector. The specimen was termed in the form of C-S-T-R, where “C” refers to the connector type (symbolized as “P” and “H” for commercial plate-type the hexagonal tube GFRP, respectively); “S” refers to the connector spacing (symbolized as “300” and “525” mm); “T” refers to the reinforcement type (symbolized as “S” and “B” for steel and BFRP rebar, respectively); and “R” refers to the longitudinal rebar diameter (symbolized as “10” and “12” mm). The flexural performance of the specimens was evaluated by four-point flexural test with a constant moment zone and shear span of 600 and 770 mm, respectively. LVDTs were placed to measure the deflection at the mid-span and loading points of the specimens. Load was applied by the hydraulic jack, as shown in Fig. 12b.



(a) Shear force vs. relative slip relationships of adopted connector (per connector)



(b) Test setup

Figure 12 Shear force vs. relative slip relationships of the adopted connectors and test setup

2D FE analysis was conducted based on ABAQUS to reproduce the tests. The FE model is seen in Fig. 13. Four-node plane stress element (CPS4R) was adopted for modelling the concrete, the XPS insulation and the loading pad. Two-node spar element (T2D2) was used for modelling the longitudinal steel and the BFRP rebar. The concrete element and the rebar element shared the same node, assuming perfect bond between them. The surface-to-surface contact interaction was used for the interfacial behaviour between the concrete and the XPS insulation. In the tangential direction, the frictionless contact was used due to the aforementioned weak bond. The GFRP connector was modelled by using spring element. Two spring elements (Spring A and B in Fig. 6.13) were adopted for modelling the axial and lateral behaviours of the connector, respectively. For Spring A, the stiffness was adopted as 128 kN/mm according to the data provided by the manufacturer. For Spring B, the average shear force vs. relative slip relationship in Fig. 12a was used to define its behaviour. The displacement-controlled mode was used for applying the load. The analysis was terminated after the load reached the peak value.

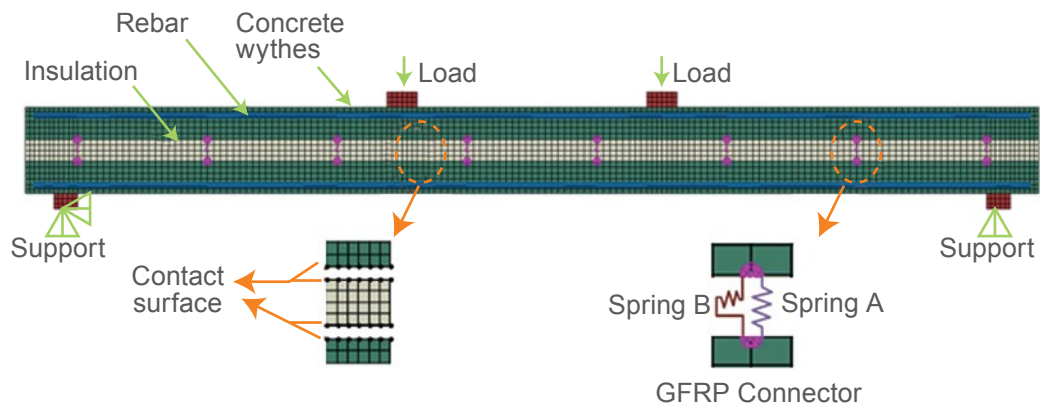
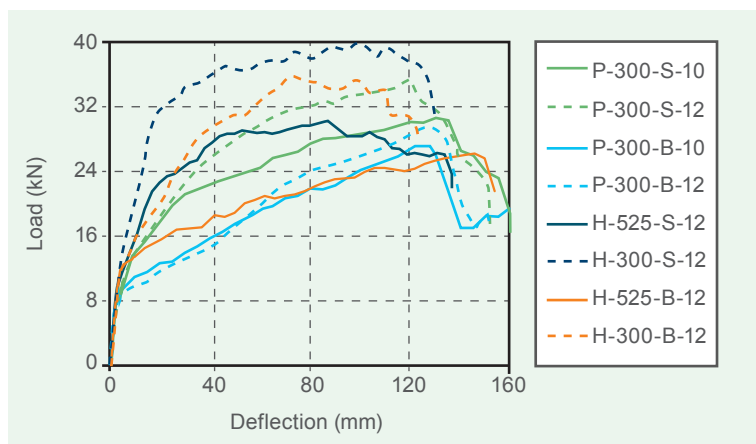


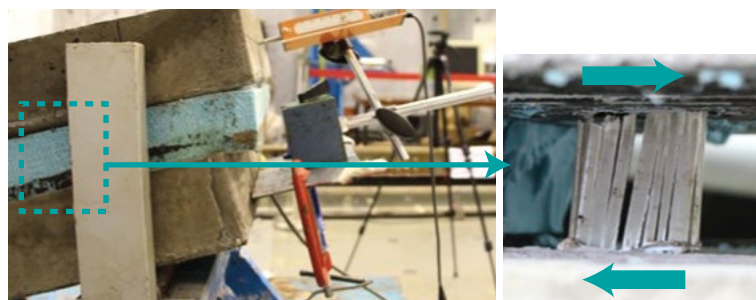
Figure 13 FE model of the PGCSP specimens

4.1.2 Results

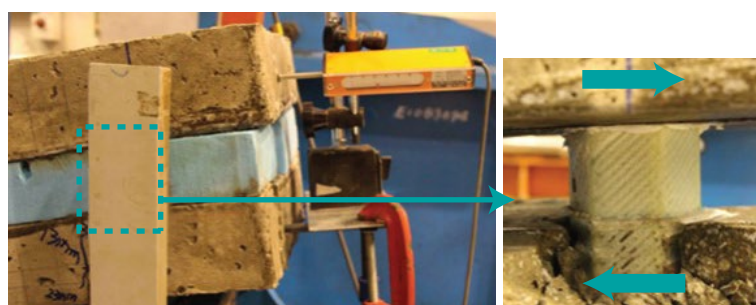
Load vs. mid-span deflection relationships of the PGCSP specimens are shown in Figure 14a. It was seen that: (1) The BFRP rebar reinforced specimens had a lower post-cracking stiffness and load carrying capacity than those of the steel rebar reinforced counterparts; (2) Based on the comparison of the four P series specimens, it was seen that the load carrying capacity of the samples increased by the increase of reinforcement ratio; (3) By comparing the curves of P-300-S-12 and P-300-B-12 with those of H-300-S-12 and H-300-B-12, it was evident that the post-cracking stiffness and load carrying capacity of the PGCSP using hexagonal tube connector were significantly higher than those with commercial plate-type connector; (4) Based on the comparison of the four H series specimens, it was seen that the post-cracking stiffness and load carrying capacity of the PGCSP would be enhanced by the decrease of connector spacing.



(a) Load vs. mid-span deflection relationship



P series specimens



H series specimens

(b) Connector at the failure stage

Figure 14 Load-deflection relationship of the PGCSP specimens and the connector at the failure stage

The connectors at the failure stage are seen in Fig. 14b. The failure modes and the crack patterns of P-300-B-12 and H-300-B-12 are shown in Fig. 15. From the figures, the failure mode of the P series specimens was governed by the connector breakage. However, in the H series, although considerable damage was seen in the GFRP laminates, the failure mode was governed by the connector pull-out.

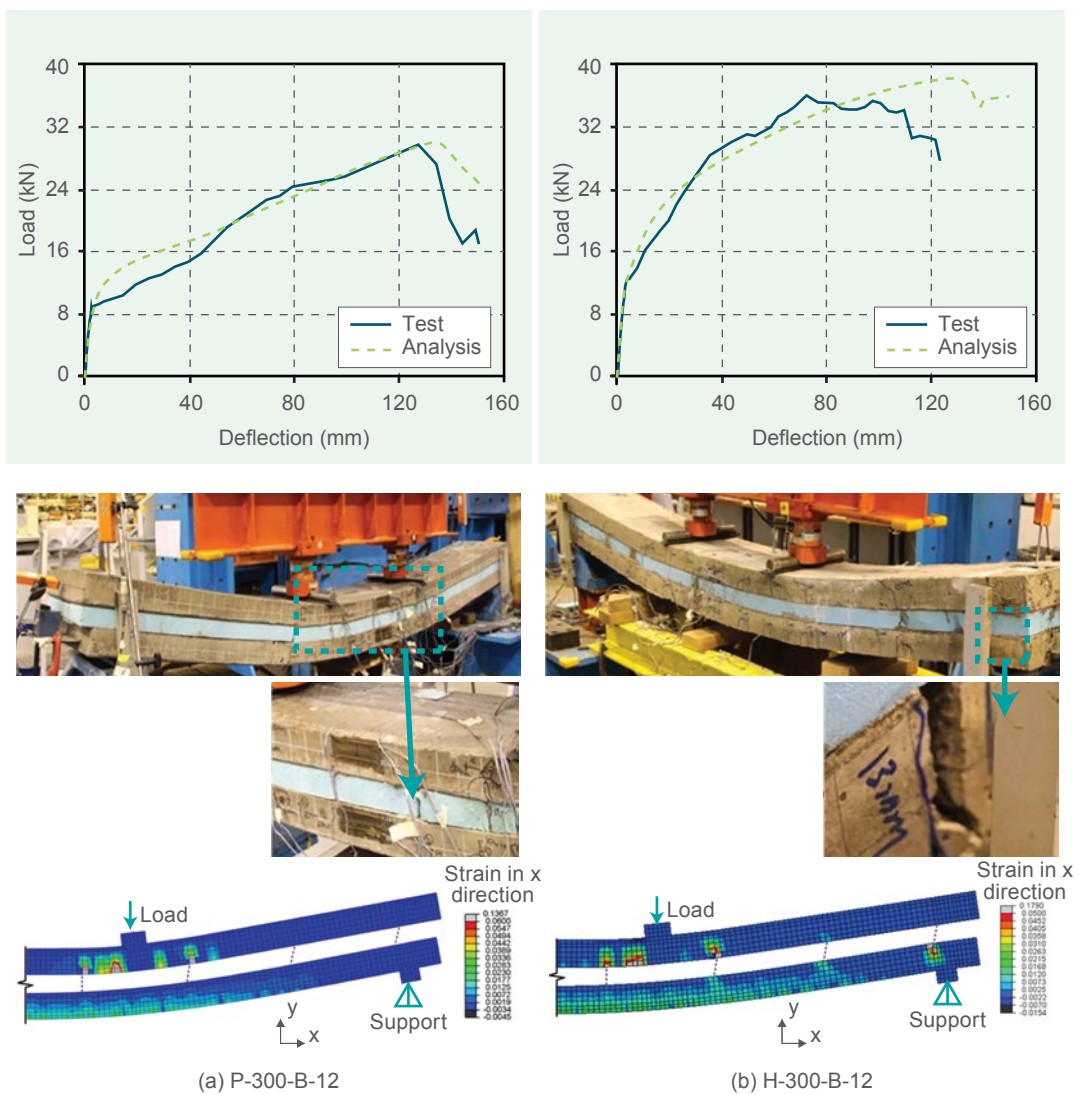


Figure 15 Comparison on the results of the PGCSFs between test and FE analysis results

The degree of composite action in terms of initial stiffness (DCA_{is}) and ultimate strength (DCA_{us}) were used to evaluate the composite action of the specimens in both pre-cracking stage and ultimate stages, respectively. DCA_{is} was obtained as $DCA_{is} = [(I_{test} - I_{nc}) / (I_{fc} - I_{nc})] \times 100\%$. In this equation, I_{test} is the moment of inertia of the test PCSP which was calculated according to the initial stage of the load-deflection curves from the tests. I_{nc} and I_{fc} are the theoretical moments of inertia of the non-composite (NC) and fully composite (FC) counterparts, respectively. DCA_{us} was obtained as $DCA_{us} = [(P_{test} - P_{nc}) / (P_{fc} - P_{nc})] \times 100\%$. P_{test} is the load carrying capacity of the tested PCSP. P_{nc} and P_{fc} are the theoretical load carrying capacities related to the NC and FC counterparts, respectively. They were obtained according to ACI-318-05 (2005) for steel reinforced PCSP and ACI 440.1R-06. (2006) for FRP reinforced PCSP. The values of calculated parameters are shown in Table 3. It was seen that by reducing the connector spacing and replacing the plate-type connector with hexagonal tube connector, both values of DCA_{is} and DCA_{us} increased. Also, reducing the reinforcement ratio increased the DCA_{us} value.

Table 3 Test values of DCA_{is} and DCA_{us}

Specimen ID	I_{test} ($\times 10^7 \text{mm}^4$)	I_{fc} and I_{nc} ($\times 10^7 \text{mm}^4$)	DCA_{is} (%)	P_{test} (kN)	P_{fc} and P_{nc} (kN)	DCA_{us} (%)
P-300-S-10	3.12	FC 19.69 NC 2.11	5.76	30.80 0	FC 28.12 NC 11.27	115.92
P-300-S-12	3.05	FC 19.69 NC 2.11	5.37	35.50 0	FC 41.09 NC 15.99	77.75
P-300-B-10	3.03	FC 19.69 NC 2.11	5.23	27.30 0	FC 71.75 NC 14.53	22.33
P-300-B-12	3.05	FC 19.69 NC 2.11	5.37	29.80 0	FC 87.52 NC 17.16	17.96
H-525-S-12	3.44	FC 19.69 NC 2.11	7.54	30.30 0	FC 41.08 NC 15.98	57.04
H-300-S-12	4.46	FC 19.69 NC 2.11	13.3 8	40.20 0	FC 41.08 NC 15.98	96.48
H-525-B-12	3.51	FC 19.69 NC 2.11	7.99	29.40 0	FC 87.44 NC 17.14	17.44
H-300-B-12	4.33	FC 19.69 NC 2.11	12.6 6	36.20 0	FC 87.44 NC 17.14	27.11

The predicted load vs. mid-span deflection relationships of P-300-B-12 and H-300-B-12 are shown in Fig. 15. Favorable agreements were observed between the tests and FE results. Besides, the strain contours of the FE models at the peak load point are shown. Here, for H-300-B-12, the stain values in the connecting point between the connector and the bottom wythe near the support were substantial. This indicated the onset of the pull-out failure. The observations agreed well with the tests. To sum up, the FE model provided reasonable predictions for the flexural performance of the tested PGCSF specimens and was applicable to further investigations.

4.2 A Simplified Approach for Stiffness and Serviceability Prediction of Precast Concrete Sandwich Panel

4.2.1 Research Methodology

A simplified approach for predicting the load-deflection relationship of the precast concrete sandwich panel (PCSP) during both pre- and post-cracking stages was proposed. In this approach, closed-form solutions based on a continuum method were developed for predicting the load-deflection relationship during the pre-cracking stage, and the cracking load. In this simplified approach, three loading conditions were considered (see Fig. 16).

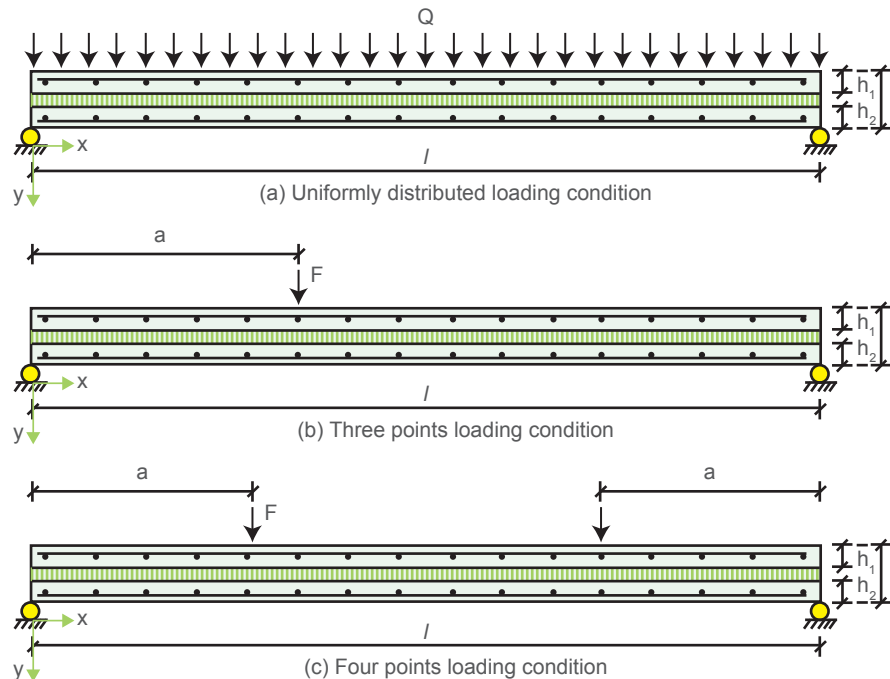


Figure 16 Loading conditions considered in the closed-form solutions

- (a) For uniformly distributed loading condition, the mid-span deflection (y_{UDL}) and the cracking load (Q_{crU}) were calculated as:

$$y_{UDL} = \frac{1}{E_c(I_1+I_2)} \left(\frac{2Q(e^{-0.5\lambda l} - e^{0.5\lambda l})}{\lambda^4(e^{-\lambda l} - e^{\lambda l})} + \frac{Q}{8\lambda^2} l^2 - \frac{Q}{\lambda^4} \right) \quad (1)$$

$$Q_{crU} = \left[\frac{h_2}{2(I_1+I_2)f_r} \left(-\frac{2(e^{-0.5\lambda l} - e^{0.5\lambda l})}{\lambda^2(e^{-\lambda l} - e^{\lambda l})} + \frac{1}{\lambda^2} \right) + \frac{1}{f_r A_2} \left(\frac{2(e^{-0.5\lambda l} - e^{0.5\lambda l})}{\lambda^2 r(e^{-\lambda l} - e^{\lambda l})} + \frac{1}{8r} l^2 - \frac{1}{\lambda^2 r} \right) \right]^{-1} \quad (2)$$

- (b) For three points loading condition, the deflection at the loading point (y_{TPL}) and the cracking load (F_{crT}) were calculated as:

$$y_{TPL} = \frac{F}{\lambda^2 E_c(I_1+I_2)} \left[\frac{(e^{\lambda a} - e^{2\lambda l - \lambda a})(e^{\lambda a} - e^{-\lambda a})}{2\lambda(e^{2\lambda l} - 1)} - \frac{(a-l)a}{l} \right] \quad (3)$$

$$F_{crT} = \left[\frac{-h_2}{2f_r(I_1+I_2)} \left(\frac{(e^{\lambda a} - e^{2\lambda l - \lambda a})}{2\lambda(e^{2\lambda l} - 1)} (e^{\lambda a} - e^{-\lambda a}) \right) + \frac{1}{f_r A_2} \left(\frac{(e^{\lambda a} - e^{2\lambda l - \lambda a})}{2\lambda r(e^{2\lambda l} - 1)} (e^{\lambda a} - e^{-\lambda a}) + \frac{a}{r} - \frac{a^2}{rl} \right) \right]^{-1} \quad (4)$$

- (c) For four points loading condition, the mid-span deflection (y_{FPL}) and the cracking load (F_{crF}) were calculated as:

$$y_{FPL} = -\frac{F(e^{\lambda a} - e^{-\lambda a})e^{0.5\lambda l}}{\lambda^3 E_c(I_1+I_2)(1+e^{\lambda l})} + \frac{Fa}{\lambda^2 E_c(I_1+I_2)} \quad (5)$$

$$F_{crF} = \left[\frac{h_2(e^{\lambda a} - e^{-\lambda a})e^{\lambda 0.5l}}{2f_r(I_1+I_2)\lambda(1+e^{\lambda l})} + \frac{a}{A_2 r f_r} - \frac{(e^{\lambda a} - e^{-\lambda a})e^{\lambda 0.5l}}{A_2 \lambda r f_r(1+e^{\lambda l})} \right]^{-1} \quad (6)$$

where I_1 and I_2 are the gross moments of inertia of the top and bottom RC wythes, respectively; h_1 and h_2 are the section thickness of top and bottom RC wythes, respectively; l is the length between two supports; a is the length of the shear span; r is the distance between the center of the two RC wythes; E_c is the concrete elastic modulus; λ is a parameter which was calculated as $\lambda = [kr^2/E_c(I_1 + I_2)]^{0.5}$, in which $k = K/S$. K is the stiffness of a connector and S is the connector spacing.

In the proposed approach, an equivalent moment of inertia (I_e) was introduced to calculate the deflection of the PCSP during post-cracking stage, as shown in the following:

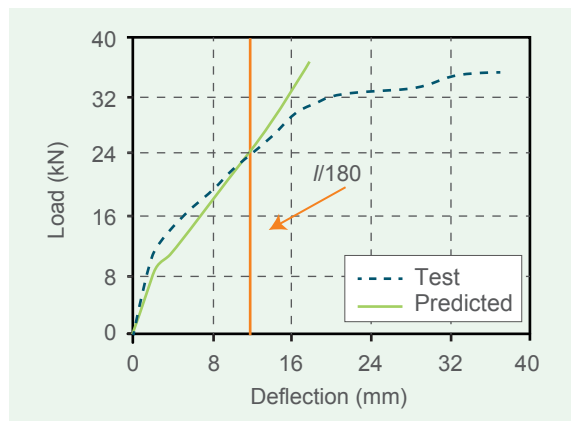
$$I_e = \left(\frac{M_{cr}}{M} \right)^3 I_g + \left[1 - \left(\frac{M_{cr}}{M} \right)^3 \right] \beta I_{cr} \quad (7)$$

where M_{cr} is the cracking moment of the PCSP; M is the applied load in the moment; I_g and I_{cr} are the gross moment of inertia and the cracked moment of inertia of the PCSP, respectively. Both I_g and I_{cr} were calculated based on the developed closed-formed solution. Also, β is a reduction factor which is equal to 1.0 for steel reinforced PCSP and 0.27 for BFRP reinforced PCSP.

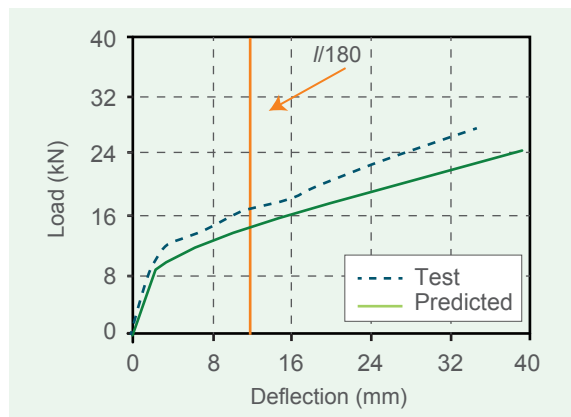
Fourteen tests were used to validate the accuracy of the proposed simplified approach, including six PCSP tests adopted from Natio *et al.* (2011) and eight PGCSPP tests previously mentioned here.

4.2.2 Results

For H-300-S-12 and H-300-B-12, the predicted load vs. mid-span deflection relationships are compared to those of tests in Fig. 17. The closed-form solution reasonably predicted the load-deflection relationship during the pre-cracking stage. For steel reinforced PCSP, by adopting the equivalent moment of inertia, a reasonable prediction of the load-deflection relationship was achieved before $l/180$ (mid-span deflection). However, after this point, the difference between the predicted and the test results was larger. This difference was caused due to the damaged connector and yielded steel rebar. For BFRP reinforced PCSP, the predicted results using the equivalent moment of inertia agreed well with the tests.



(a) H-300-S-12



(b) H-300-B-12

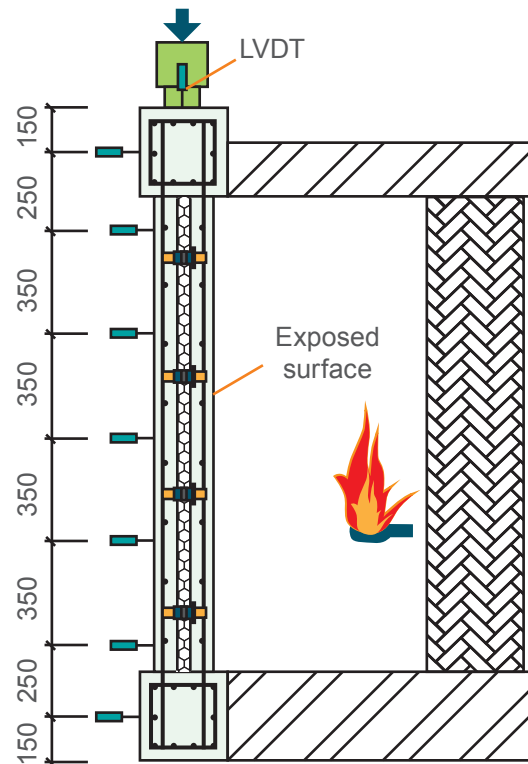
Figure 17 Comparisons of load vs. mid-span deflection relationships between test and simplified approach

5 FIRE PERFORMANCE OF PRECAST GEOPOLYMER CONCRETE SANDWICH PANELS

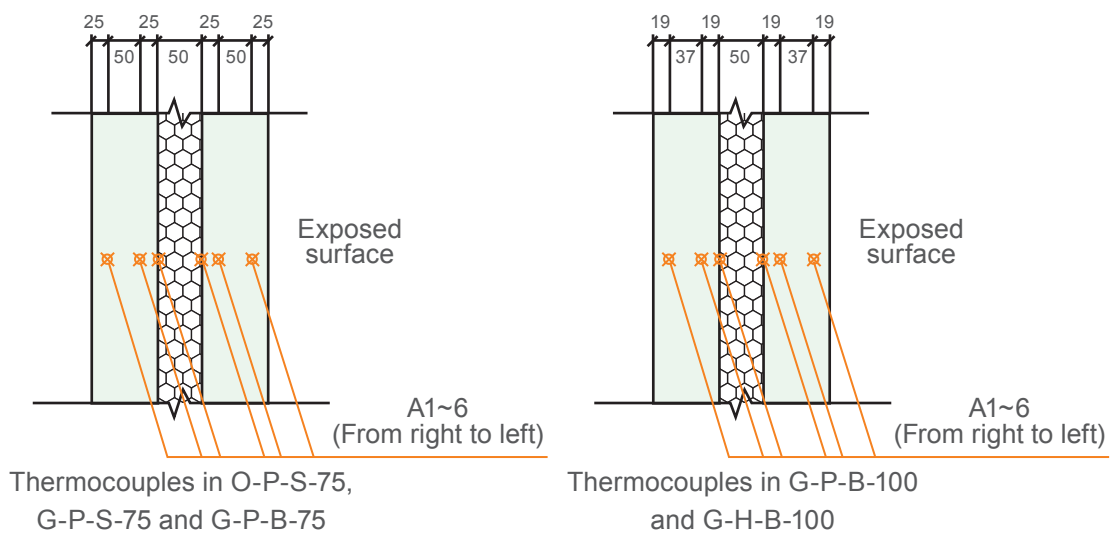
5.1 Research Methodology

The fire performance of the PGCSP was evaluated experimentally. In total, five PCSP specimens were fabricated and tested under one-side fire condition. The dimensions of the specimens were 1600×900×200 mm or 1600×900×250 mm (height×width×thickness). The outer concrete wythe was 75 or 100 mm thick, and the core XPS insulation was 50 mm thick. The investigated parameters included the concrete type (geopolymer and OPC concrete), the reinforcement type (steel and BFRP rebar), the connector type (plate-type and hexagonal tube GFRP), and the concrete wythe thickness (75 and 100 mm). Reinforced concrete (RC) beams with the dimensions of 300×300×900 mm (width×height×length) were fabricated at the top and the bottom of the PCSP for transferring forces. The specimens were termed in the form of C-S-T-W, where “C” refers to the concrete type (symbolized as “G” and “O” for geopolymer and OPC concrete, respectively); “S” refers to the connector type (symbolized as “P” and “H” for commercial plate-type the hexagonal tube GFRP, respectively); “T” refers to the reinforcement type (symbolized as “S” and “B” for steel and BFRP rebar, respectively); and “W” refers to the concrete wythes thickness (symbolized as “75” and “100” mm). The testing procedure was divided into two phases. Firstly, the axial compressive load was applied to the top RC beams, aiming to reach an axial load ratio of 0.15. Thereafter, one surface of the PCSP was exposed to fire in the furnace as shown in Fig. 18a. The furnace temperature was controlled based on the ISO-834 standard fire curve.

The test was terminated after a fire duration of 240 min. The furnace could not withstand longer durations. To measure the temperatures of the concrete within the cross section, 6 thermocouples were mounted at different depths of the specimen center as shown in Fig. 18b. These thermocouples were marked as A1~6. LVDTs were used to measure the axial displacements (see Fig. 18a).



(a) Test setup

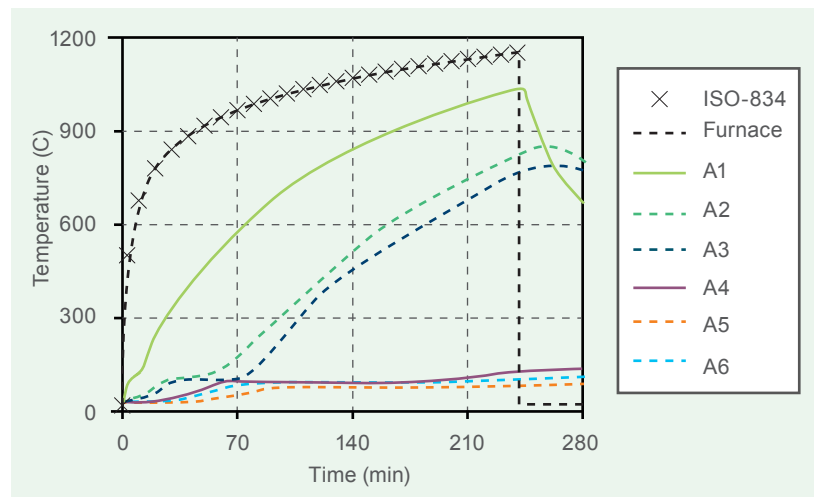


(b) Location of the thermocouples

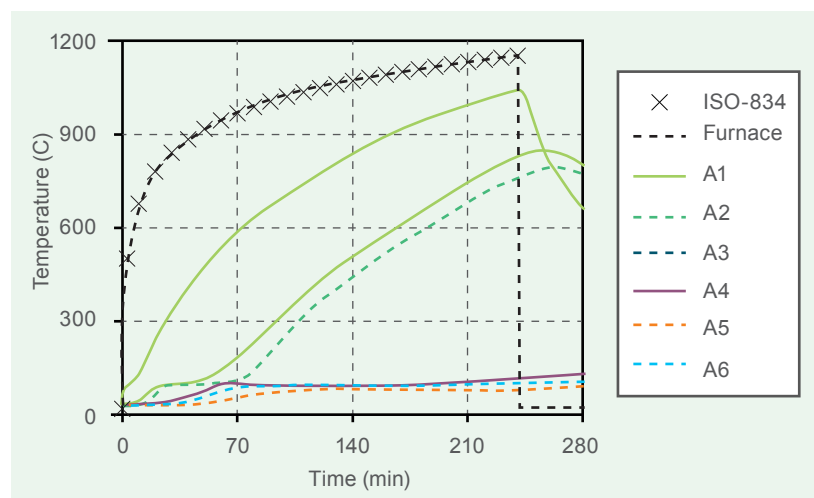
Figure 18 Test setup and the location of the thermocouples (unit: mm)

5.2 Results

The temperature distributions and failure mode of the O-P-S-75 and G-P-S-75 were shown in Fig. 19. Besides, the relationships between axial displacement and fire duration of all specimens are seen in Fig. 20. It was found that: (1) the temperature distributions of PGCSPPs and the OPC concrete counterpart were similar; (2) the failure mode of the PCSP with the OPC concrete was characterized by concrete crushing on the concrete wythe at the heating side, and (3) the PGCSPP specimens exhibited higher fire resistance than the OPC concrete counterparts. From the tests, the fire resistance of the OPC concrete specimen was 234 min, whereas the fire resistances of all PGCSPP specimens were higher than 240 min.



(a) Temperature distribution of O-P-S-75



(b) Temperature distribution of G-P-S-75



(c) Failure mode of O-P-S-75

(d) Failure mode of G-P-S-75

Figure 19 Temperature distributions and failure mode of the O-P-S-75 and G-P-S-75

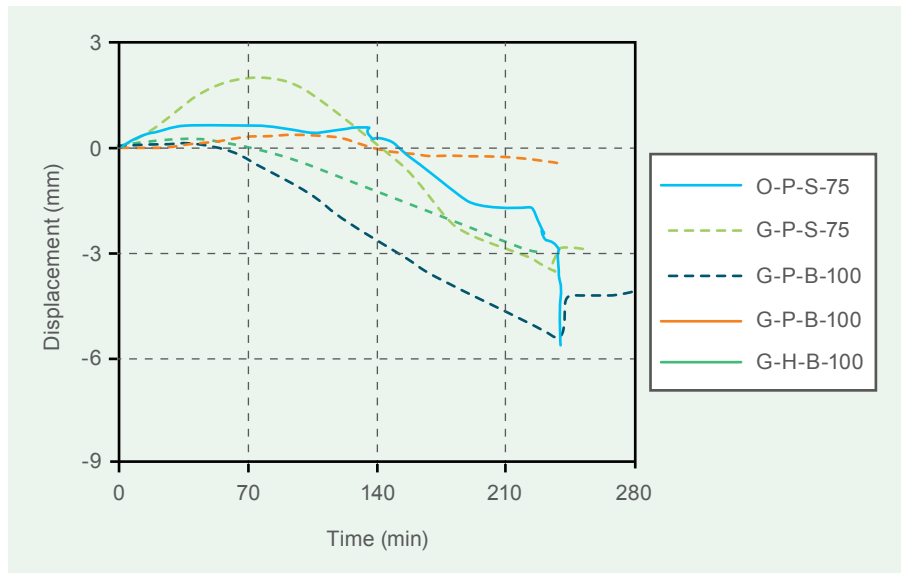


Figure 20 Relationships between axial displacement and fire duration

6 CONCLUSIONS AND FURTHER RESEARCH

6.1 Conclusions

For the development of the new type of GFRP connector and the performance characterization, it was concluded that: (1) all connectors reflected a progressive failure; (2) for a lower GFRP laminate thickness, the flat plate connector exhibited less deformability than the corrugated one due to the buckling of the laminate. Increasing the GFRP laminate thickness helped to avoid such buckling and improved the deformability; and (3) the hexagonal tube connector performed similarly along two orthogonal directions, indicating its excellent potential for use in PCSPs as a two-way connector.

For the structural performance of steel and FRP-reinforced geopolymer concrete one-way slabs, it was concluded that: (1) the flexural performances of the steel reinforced geopolymer concrete one-way slabs and the OPC concrete counterparts were similar; (2) the design provisions (i.e., ACI 318-05 and GB-50010-2010) had the potential to be used for predicting the cracking load and the load carrying capacity of the steel reinforced geopolymer concrete one-way slabs; (3) the failure of all the tested BFRP reinforced geopolymer concrete one-way slabs was governed by shear-compression. Also, a similar shear resistance was obtained for them; and (4) the equation in JSCE shear design method was recommended for use in calculating the shear resistance of the BFRP reinforced geopolymer concrete one-way slabs.

For the structural performance of PGCSPs and the simplified approach for stiffness and serviceability prediction, it was concluded that: (1) the post-cracking stiffness and the load carrying capacity of BFRP reinforced PGCSP specimens were lower than those of the steel reinforced counterparts; (2) the failure modes of the PGCSP specimens with the plate-type and hexagonal tube GFRP connector were governed by the connector breakage and connector pull-out, respectively; (3) replacing the commercial plate-type GFRP connector by the hexagonal tube GFRP connector significantly increased the degree of composite action in terms of both stiffness and strength. Also, reducing the spacing of hexagonal tube GFRP connectors further increased these two values, indicating a good potential for the developed PCSP system in practical engineering; and (4) the simplified approach gave an accurate prediction of the load-deflection relationship for a PCSP under out-of-plane load, indicating a good potential for use in design of PCSP.

For the fire performance of the PGCSP, it was concluded that (1) the PGCSP reflected similar temperature distribution with the OPC concrete counterpart; and (2) the PGCSP specimens exhibited higher fire resistance than the OPC concrete counterparts.

6.2 Further Research

This report was primarily concerned with the performance of a newly developed PCSP system. The research presented here was significantly advanced in terms of the understanding in this field but much further research is still needed for the safe and reliable application of this PCSP system in practical engineering.

Firstly, the performance of other two-way FRP connectors should be investigated. In this report, according to the existing lab facilities and considering the manufacturing convenience, the hexagonal tube GFRP connector was selected to test. Whether this section type is an optimal choice remains unknown. Therefore, in further research, an experimental investigation should be conducted to study the effect of section type (e.g. rectangular, pentagonal, hexagonal and circular tube) on the individual performance of the tubular FRP connector.

Secondly, the proposed simplified approach for predicting the deflection of BFRP reinforced PCSP needs further verifications. It was noted that the stiffness degradation of the BFRP reinforced PCSP in the post-cracking stage was a complicated phenomenon. The proposed approach was validated by limited test results in this report. In further research, more experimental studies are needed for verification purpose.

Finally, details of the connection between the proposed PCSP system and other structural members e.g., beam need to be developed and the performance of the assembled structure need to be evaluated by further experimental studies.

7 REFERENCES

- ACI 318-05 (2005). Building Code Requirements for Reinforced Concrete and Commentary, American Concrete Institute, Farmington Hills, Michigan, USA.
- ACI 440.1R-06. (2006). Guide for the design and construction of structural concrete reinforced with FRP bars, American Concrete Institute, Farmington Hills, Michigan, USA.
- Al-mahaidi, R., Zhao, X.L., Smith, S.T., and Bai, Y. (2013). "Structural performance of new thin-walled concrete sandwich wall panel system reinforced with BFRP shear connectors." *Proceedings of 4th Asia-Pacific Conference on FRP in Structures (APFIS2013)*, Swinburne University of Technology, Hawthorn, VIC, Australia.
- ASHRAE. (2005). ASHRAE Handbook – Fundamentals. Atlanta, GA: ASHRAE.
- Bush, T.D. and Stine, G.L. (1994) "Flexural behavior of composite precast concrete sandwich panels with continuous truss connectors", *PCI Journal*, 39(2): 112-121.
- Bush, T.D. and Wu, Z. (1998) "Flexural analysis of prestressed concrete sandwich panels with truss connectors", *PCI Journal*, 43(5): 76-86.
- CSA S806-12. (2012). Design and construction of building structures with fibre-reinforced polymers. Canadian Standards Association, Mississauga, Ontario, Canada.
- Davidovits, J. (1991). Geopolymers. *Journal of Thermal Analysis*, 37(8), 1633-1656.
- Duxson, P., Provis, J. L., Lukey, G. C., and Van Deventer, J. S. J. (2007). The role of inorganic polymer technology in the development of 'green concrete'. *Cement and Concrete Research*, 37(12), 1590-1597.
- Einea, A., Salmon, D.C., Tadros, M.K. and Culp, T. (1994) "A new structurally and thermally efficient precast sandwich panel system", *PCI journal*, 39(4), 90-101.
- Fernándezjiménez, A. M., Lópezhombros, C., and Palomo, A. (2006). Engineering properties of alkali-activated fly ash concrete. *ACI Materials Journal*, 103(2), 106-112.
- Frankl, B.A., Lucier, G.W., Hassan, T.K. and Rizkalla, S.H. (2011). "Behavior of precast, prestressed concrete sandwich wall panels reinforced with CFRP shear grid", *PCI Journal*, 56(2), 42-54.
- GB 50010-2010. (2010) Code for design of concrete structures, China Structural Science Academe, Beijing, China
- Hassan, T.K., Rizkalla, S.H., (2010) "Analysis and design guidelines of precast prestressed concrete, composite load-bearing sandwich wall panels reinforced with CFRP grid", *PCI journal*, 55(2), 147-162.

Hodicky, K., Sopal, G., Rizkalla, S., Hulin, T., Stang, H. (2015) "Experimental and Numerical Investigation of the FRP Shear Mechanism for Concrete Sandwich Panels", *Journal of Composites for Construction*, 19(5), 04014083.

JSCE (Japan Society of Civil Engineers). (1997). Recommendation for design and construction of concrete structures using continuous fiber reinforcing materials. Tokyo.

Lacerda, M. M. S., Silva, T. J. D., Alva, G. M. S., and Lima, M. C. V. D. (2018). Influence of the vertical grouting in the interface between corbel and beam in beam-to-column connections of precast concrete structures – an experimental analysis. *Engineering Structures*, 172, 201-213.

Naito, C. J., Hoemann, J. M., Shull, J. S., Saucier, A., Salim, H. A., Bewick, B. T., and Hammons, M. I. (2011). *Precast/prestressed concrete experiments performance on non-load bearing sandwich wall panels*. BLACK AND VEATCH OVERLAND PARK KS.

Naito, C., Hoemann, J., Beacraft, M., Bewick, B. (2012) "Performance and characterization of shear ties for use in insulated precast concrete sandwich wall panels", *Journal of Structural Engineering*, 138(1), 52-61.

Pantelides, C.P., Surapaneni, R. and Reaveley, L.D. (2008). "Structural performance of hybrid GFRP/steel concrete sandwich panels", *Journal of Composites for Construction*, 12(5), 570-576.

PCI committee. (2011). State of the art of precast/prestressed concrete sandwich wall panels. *PCI Journal*, 56(2), 131-176.

Provis, J. L., & Van Deventer, J. S. J. (2009). *Geopolymers: Structures, processing, properties and industrial applications*. CRC Press.

Woltman, G., Tomlinson, D. and Fam, A. (2013). "Investigation of various GFRP shear connectors for insulated precast concrete sandwich wall panels", *Journal of Composites for Construction*, 17(5), 711-721.

APPENDIX

Brief Guideline for Design of Precast Geopolymer Concrete Sandwich Panel Reinforced by BFRP Rebar

A brief guideline for design of the precast geopolymer concrete sandwich panel (PGCSP) reinforced by BFRP rebar was introduced in this appendix. The flow chart of the design step is shown in Fig. A1. This brief design guideline mainly focused on the PGCSP where the out-of-plane load is the main external load (i.e., façade wall and floor slab).

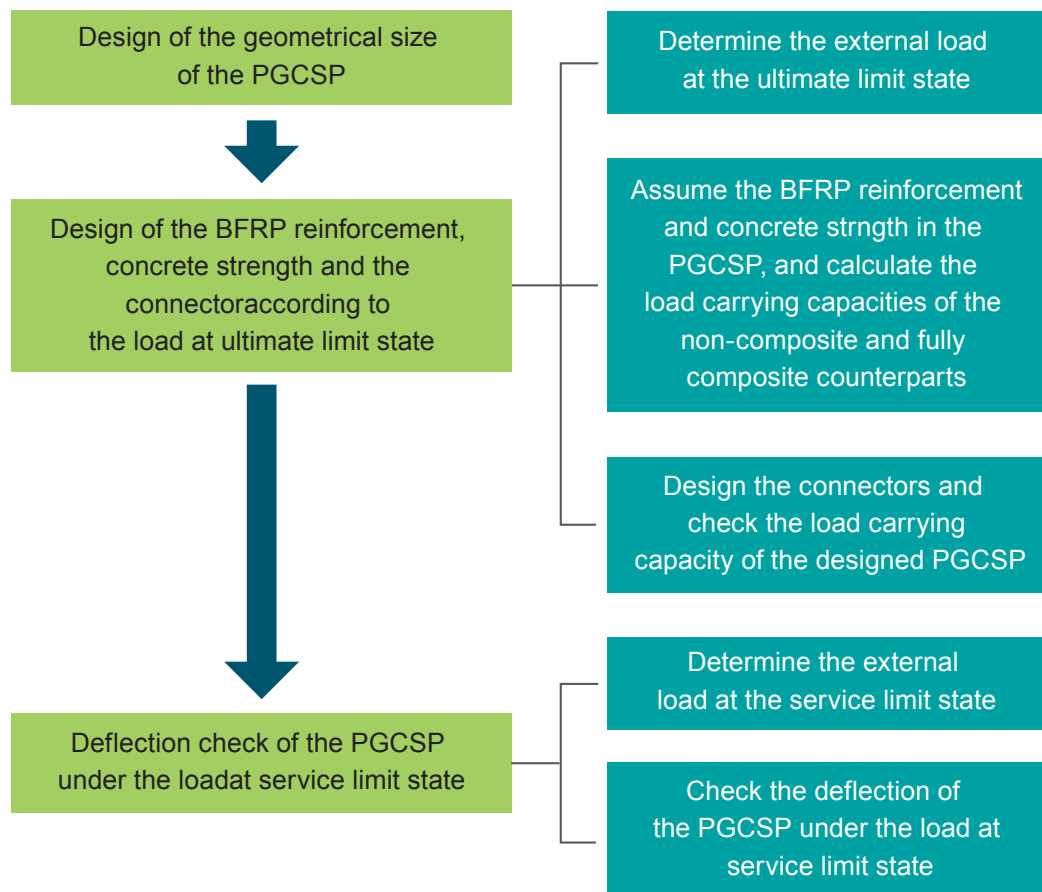


Figure A1 Flow chart of the design step

1 Design of the geometrical size of the PGCSP

The length and width of a PGCSP could be determined firstly. For the thickness of PGCSP, based on the existing research, the minimum size of 200 mm was recommended. The geopolymer concrete wythe was recommended to be larger than 75 mm to ensure a proper fire resistance. The core insulation is the key part for improving the energy efficiency of the whole panel, and the thickness could be calculated according to the required thermal resistance (i.e., R-value). The calculation procedures is referred to ASHRAE (2005). In addition, the thickness of the insulation was recommended to be larger than 50 mm.

2 Design of the BFRP reinforcement, concrete strength and the connector according to the load at ultimate limit state

This step consisted of three sub-steps as follows

(a) Determine the external load at the ultimate limit state.

The external load at the ultimate limit state was calculated according to the design code.

(b) Assume the BFRP reinforcement and concrete strength in the PGCSP, and calculate the load carrying capacities of the non-composite and fully composite counterparts.

Both non-composite and fully composite counterparts should be designed as over-reinforced. The balance reinforcement ratio, and the load carrying capacities were calculated according to ACI 440.1R-06. (2006).

(c) Design the connectors and check the load carrying capacity of the designed PGCSP

In this sub-step, the connector should be selected and the connector spacing should be determined firstly. Here, the resistance and spacing of each connector could be obtained by the manufacturer. For example, the resistance and the recommended connector spacing of the plate-type GFRP connector manufactured by Thermomass Co. Ltd. were 15 kN and 300 mm, respectively. For the developed hexagonal tube GFRP connector in this report, the resistance and the recommended connector spacing were 24 kN and 300~525 mm, respectively.

Thereafter, the degree of composite action in terms of ultimate strength (DCA_{us}) of the designed PGCSP could be estimated as $DCA_{us} = 0.8P_c/P_r$. This was summarized according to the test results in this report. Here, P_c is the total resistance provided by the connector along the shear span; $P_r = f_u \times A_s$, where f_u is the rupture strength of the BFRP rebar and A_s is the total longitudinal reinforcement area of the BFRP rebar in each wythe.

Also, it was seen that $DCA_{us} = [(P_{design} - P_{nc}) / (P_{fc} - P_{nc})] \times 100\%$, where P_{design} , P_{nc} and P_{fc} are the load carrying capacities of the designed PGCSP, non-composite counterpart and fully composite counterpart, respectively. Thus, the load carrying capacity of the designed PGCSP could be obtained afterwards. The obtained load carrying capacity of the designed PGCSP should be checked and should be higher than the external load at the ultimate limit state.

3 Deflection check of the PGCSP under the load at service limit state

This step consisted of two sub-steps as follows:

(a) Determine the external load at the service limit state

The external load at the service limit state should be calculated firstly according to the design code.

(b) Check the deflection of the PGCSP under the load at service limit state.

In this sub-step, the developed simplified approach in this report could be adopted to check the deflection of the PGCSP under the load at service limit state.



Members of CIC Task Force on Research

Mr. Jimmy TSE
Prof. Christopher LEUNG
Ir Joseph MAK
Prof. James PONG
Prof. Sze-chun WONG
Ir Chi-chiu CHAN
Mr. Shu-jie PAN

Research Team

Principal Investigator

Jian-Guo DAI

建造業議會

Construction Industry Council

Address 地址：38/F, COS Centre, 56 Tsun Yip Street, Kwun Tong, Kowloon
九龍觀塘駿業街56號中海日升中心38樓

Tel 電話：(852) 2100 9000

Fax 傳真：(852) 2100 9090

Email 電郵：enquiry@cic.hk

Website 網址：www.cic.hk



[cic_hk](#)



[HKCIC](#)



[Construction Industry Council](#)



[CICHK](#)



[HKCIC](#)



[Construction Industry Council Hong Kong](#)

Copyright © Construction Industry Council

All rights reserved. No part of this publication may be reproduced, stored in a retrieval system, or transmitted in any form or by any means, electronic, mechanical, photocopying, recording or otherwise, without the prior written permission of the publisher

2018

CIC Research Report No. CICRS_019